Behavioral/Systems/Cognitive

Distinct Firing Patterns of Identified Basket and Dendrite-Targeting Interneurons in the Prefrontal Cortex during Hippocampal Theta and Local Spindle Oscillations

Katja Hartwich, Thomas Pollak, and Thomas Klausberger

Medical Research Council Anatomical Neuropharmacology Unit, Department of Pharmacology, Oxford University, Oxford OX1 3TH, United Kingdom, and Center for Brain Research, Medical University of Vienna, 1090 Vienna, Austria

The medial prefrontal cortex is involved in working memory and executive control. However, the collective spatiotemporal organization of the cellular network has not been possible to explain during different brain states. We show that pyramidal cells in the prelimbic cortex fire synchronized to hippocampal theta and local spindle oscillations in anesthetized rats. To identify which types of interneurons contribute to the synchronized activity, we recorded and juxtacellularly labeled parvalbumin- and calbindin-expressing (PV+/CB+) basket cells and CB-expressing, PV-negative (CB+/PV−) dendrite-targeting interneurons during both network oscillations. All CB+/PV− dendrite-targeting cells strongly decreased their firing rate during hippocampal theta oscillations. Most PV+/CB+ basket cells fired at the peak of dorsal CA1 theta cycles, similar to prefrontal pyramidal cells. We show that pyramidal cells in the ventral hippocampus also fire around the peak of dorsal CA1 theta cycles, in contrast to previously reported dorsal hippocampal pyramidal cells. Therefore, prefrontal neurons might be driven by monosynaptic connections from the ventral hippocampus during theta oscillations. During prefrontal spindle oscillations, the majority of pyramidal cells and PV+/CB+ basket cells fired preferentially at the trough and early ascending phase, but CB+/PV− dendrite-targeting cells fired uniformly at all phases. We conclude that PV+/CB+ basket cells contribute to rhythmic responses of prefrontal pyramidal cells in relation to hippocampal and thalamic inputs and CB+/PV− dendrite-targeting cells modulate the excitability of dendrites and spines regardless of these field rhythms. Distinct classes of GABAergic interneuron in the prefrontal cortex contribute differentially to the synchronization of pyramidal cells during network oscillations.

Introduction

The mammalian neocortex contains a large diversity of neurons forming functionally specialized and highly interconnected networks. The majority of cortical neurons are glutamatergic pyramidal cells, which have both local and long-range axonal projections. Only 20 to 30% of neocortical neurons are GABAergic interneurons (Beaulieu and Somogyi, 1990; DeFelipe, 1993) with locally concentrated axons. Interneurons are heterogeneous in their postsynaptic targets, molecular expression, and temporal activity (Freund and Buzsaki, 1996; Kawaguchi and Kubota, 1997; Kisvárday et al., 1997; Swadlow et al., 1998; Cauli et al., 2000; Gupta et al., 2000; Markram et al., 2004; Tamas et al., 2004; Bacci et al., 2005; Földy et al., 2005; Krimer et al., 2005; Dumitriu et al., 2007; Kapfer et al., 2007; Ali and Thomson, 2008; Ascoli et al., 2008; Galarreta et al., 2008; Klausberger and Somogyi, 2008; Helmstaedter et al., 2009). Interneurons play a key role in regulating the organization and dynamics of cortical circuits. They precisely control the firing of pyramidal cells and also contribute to rhythmic cortical activity at different oscillatory frequencies (Buzsáki and Draguhn, 2004), which supports the transfer and processing of information within and between cortical structures (Engel and Singer, 2001).

The medial prefrontal cortex (mPFC) is involved in the cognitive control of working memory, planning and decision-making (Miller, 2000; Fuster, 2001; Jones, 2002; Dalley et al., 2004; Vertes, 2006; Euston et al., 2007). The mPFC receives monosynaptic glutamatergic inputs from many brain structures including the mediodorsal thalamus (Krettek and Price, 1977; Giguere and Goldman-Rakic, 1988) and the CA1 area and subiculum of the hippocampus (Swanson, 1981; Jay and Witter, 1991; Cenquizca and Swanson, 2007; Hoover and Vertes, 2007) innervating both pyramidal cells and interneurons (Gabbott et al., 2002; Kuroda et al., 2004; Tierney et al., 2004; Rotaru et al., 2005).

Theta oscillations (4–10 Hz) occur in the hippocampus during exploration and REM sleep (Buzsaki, 2002). Simultaneous recordings from the hippocampus and prefrontal cortex have demonstrated that some prefrontal neurons fire in synchrony with the hippocampal theta rhythm (Siapas et al., 2005), and spike timing and theta oscillations become more coordinated during epochs requiring spatial working memory and decision making (Jones and Wilson, 2005). Spindle oscillations (7–14 Hz) occur synchronously over widespread thalamic and neocortical

Received March 24, 2009; revised May 23, 2009; accepted June 22, 2009.

This work was supported by Grant P16637 of the Austrian Science Fund. We thank Klara Peto, Wai-Yee Suen, Ben Micklem, and Kristina Detzner for expert technical assistance; John Tukker, Judy Creso, John Huxter, and Stephen Ellis for advice on computational analysis; and Peter Somogyi, Balint Lasztoczi, Nico Mallet, and Peter Magill for commenting on an earlier version of this manuscript.

Correspondence should be addressed to Thomas Klausberger, Medical Research Council Anatomical Neuropharmacology Unit, Department of Pharmacology, Oxford University, Oxford OX1 3TH, UK. E-mail: thomas.klausberger@pharm.ox.ac.uk.

DOI:10.1523/JNEUROSCI.1397-09.2009

 0270-6474/09/299563-12$15.00/0

areas during non-REM sleep (Contreras, 1997; Hugenard and McCormick, 2007). Spindles are generated through interactions of thalamic reticular neurons with thalamocortical neurons (Steriade et al., 1993). They are temporally organized by simultaneously occurring slower (~1 Hz) oscillations (Steriade et al., 1993; Sanchez-Vives and McCormick, 2000; Mölle et al., 2002). Spindle and slow oscillations have been linked to memory consolidation processes (Siapas and Wilson, 1998; Sirota et al., 2003) in which hippocampal information is transferred to the neocortex. However, in contrast to the growing knowledge of the contribution of pyramidal cells, little is known about the activity of cortical interneurons.

To understand the cellular mechanisms of network oscillations in the mPFC, we determined the spatiotemporal relationship of identified GABAergic interneurons and pyramidal cells in the prelimbic (PL) area of the mPFC during hippocampal theta and local spindle oscillations *in vivo*.

Materials and Methods

Extracellular recording and labeling. Experimental procedures were performed on adult male Sprague Dawley rats (250–350 g) and were conducted in accordance with the Animals (Scientific Procedures) Act, 1986 (United Kingdom) and associated procedures, and with the Society for Neuroscience Policies on the Use of Animals in Neuroscience Research.

Anesthesia was induced with isoflurane and maintained with urethane (1.25 g/kg of body weight; i.p.) and supplemental doses of ketamine and xylazine (20 and 2 mg/kg, respectively; i.p.) as required. All wound margins were locally treated with marcain. During the whole experiment, body temperature was maintained at 37°C and electrocardiographic activity was constantly monitored to ensure the animals' wellbeing.

The neuronal activity was recorded extracellularly and simultaneously in the PL area of the mPFC (coordinates relative to bregma: anteroposterior, +3.4 mm; mediolateral, −0.3 mm; dorsoventral, 2.4–3.5 mm) and in the CA1 area of the dorsal hippocampus (coordinates relative to bregma: anteroposterior, −3.6 mm; mediolateral, −2.3 mm; dorsoventral, ~2.4 mm) (Paxinos and Watson, 2007). In the CA1 area, the local field potential (LFP) was always recorded in stratum pyramidale or stratum oriens with a single glass electrode filled with 1.5% neurobiotin in 0.5 M NaCl (12–25 MΩ, tip diameter ~1.5 μm). Only those recordings were included in which the position of the glass electrode was identified by electrophysiological characteristics including large-amplitude regular theta oscillations and the occurrence of sharp wave-associated ripples with a positive deflection (Tukker et al., 2007); the firing of CA1 pyramidal cells was used for orientation. In three experiments the location of the dorsal CA1 theta detection site was confirmed by recording and labeling a neuron with this electrode. Two neurons were located in stratum oriens and one was located at the stratum oriens/pyramidale border of the dorsal CA1 area. In two animals, prefrontal multiunit activity and LFP were recorded with four tetrodes (separated in the anteroposterior axis by ~200 μm) targeting layers II–V of the PL cortex. After the first recording session, the tetrodes were lowered together by at least 200 μm to obtain a new set of units.

Tetrodes were made of four twisted 13 μm enamel-coated nichrome wires (200–300 kΩ) and attached to a 16 channel acute head stage (RA16AC, Tucker-Davis Technologies). Tetrode signals were referenced against a screw implanted above the contralateral cerebellum, amplified (1000×) and wide-band recorded (0–6000 Hz) using programmable differential amplifiers (Lynx-8, Neuralynx),

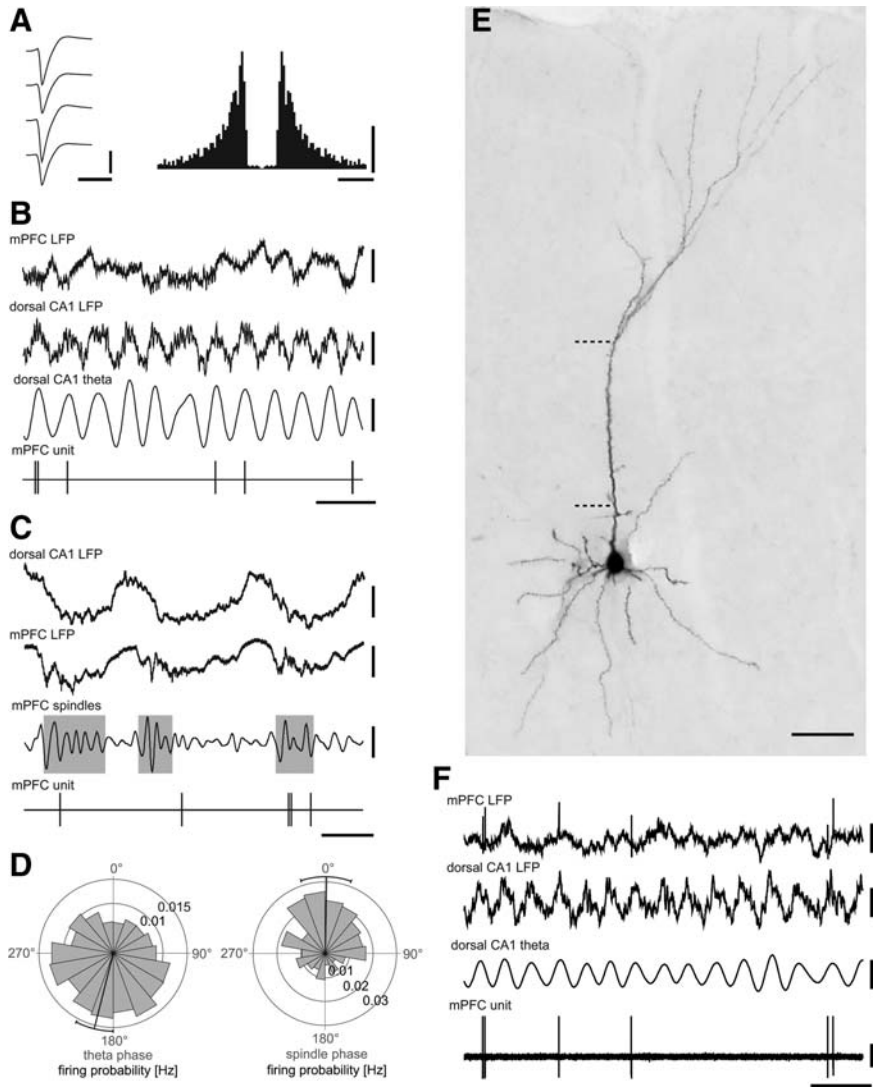

Figure 1. *In vivo* firing patterns of a putative pyramidal cell and an identified pyramidal cell in the prefrontal cortex during hippocampal theta and local spindle oscillations. ***A***, Average wide-band signals of extracellular action potentials fired by a single neuron as recorded from a wire tetrode (left) and autocorrelogram of action potentials (right). ***B***, This prefrontal cell often fired at the peak of theta oscillations recorded extracellularly from the pyramidal cell layer of the dorsal CA1 hippocampus (third trace, filtered 3–6 Hz); note that theta oscillations in the LFP of the mPFC (first trace) were less pronounced compared with those in the hippocampus (second trace). ***C***, The cell fired at the negative phase of the 1 Hz oscillations recorded extracellularly from the same wire tetrode (second trace). During simultaneously occurring spindle oscillations (gray boxes; filtered 7–14 Hz), the cell fired preferentially at the trough. Slow 1 Hz oscillations can also be seen in the hippocampus (first trace). ***D***, Firing probability of the prefrontal cell during CA1 theta oscillations (left) and local spindle oscillations (right); 0° and 180° mark the trough and the peak of the cycles, respectively; black lines show the mean angles with their 95% confidence interval. ***E***, Immunofluorescence micrograph showing the soma and dendrites of an extracellular recorded and neurobiotin-labeled layer III pyramidal cell. The dashed lines mark the boarder to layer II (bottom) and layer I (top). ***F***, This identified cell fired preferentially around the peak of theta oscillations recorded in the pyramidal layer of the dorsal CA1. Calibrations: ***A***, left, 0.04 mV and 1.6 ms; right, 50 spikes and 10 ms; ***B***, mPFC LFP, CA1 LFP, and CA1 theta, 0.5 mV, 0.5 s; ***C***, CA1 LFP, mPFC LFP, and mPFC spindles, 0.5 mV, 0.5 s; ***F***, mPFC LFP, CA1 LFP, CA1 theta, mPFC unit, 0.5 mV; 0.5 s. Scale bar in ***E***: 50 μm.

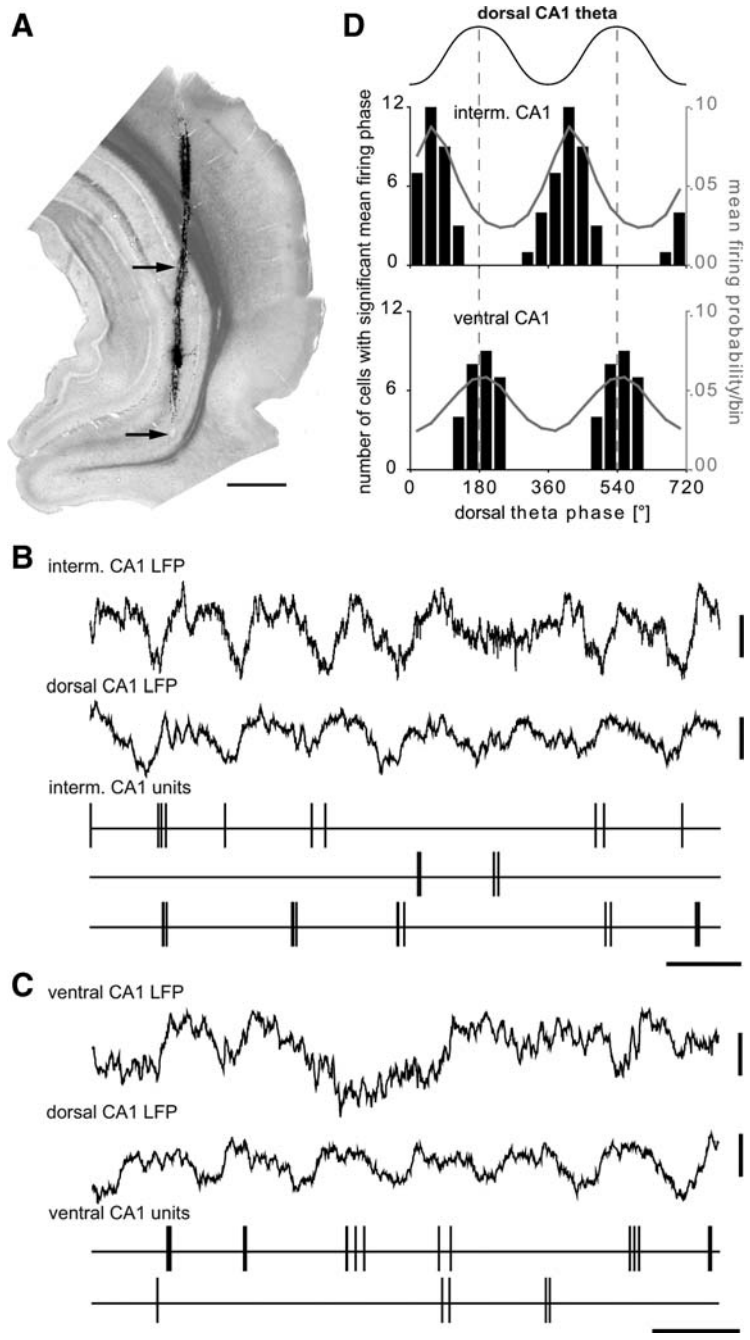

Figure 2. Firing of putative pyramidal cells of the intermediate and ventral CA1 hippocampus relative to theta oscillations recorded in the dorsal CA1. ***A***, Light micrograph (stack of 4 consecutive sections with 70 μm thickness) showing the tetrode track stained with DiI. The two arrows point to the recording sites in the intermediate and ventral CA1 pyramidal layer with traces shown in ***B*** and ***C***, respectively. Scale bar, 1 mm. ***B***, Thirty-six putative pyramidal cells in the intermediate CA1 area (recorded from 4 rats and 6 sites) fire preferentially at the early ascending phase of the theta oscillations recorded in the pyramidal layer of the dorsal CA1 area (second trace). ***C***, Twenty-eight putative pyramidal cells of the ventral CA1 area (recorded from 5 rats and 10 sites) fire preferentially to the peak of the dorsal theta cycle. Note that theta oscillations recorded in the ventral CA1 are less regular then in the dorsal CA1 and slightly phase shifted. Calibration: all CA1 LFP, 0.3 mV; all CA1 units, marker, 0.2 s. ***D***, Upper schematic waveform indicates two theta cycles; 0° and 360° mark the troughs. The black columns and left *y*-axis indicate the number of putative pyramidal cells observed with a significant mean firing phase. The gray curve and right *y*-axis indicate the mean firing probability of all putative pyramidal cells. Note that pyramidal cells in the intermediate CA1 area are modulated in time to the early ascending phase of the dorsal CA1 theta cycle and pyramidal cells in the ventral CA1 area fire preferentially around the peak of dorsal CA1 theta. interm., Intermediate.

and digitized with a 16 bit resolution and a sampling rate of 20 kHz using an analog-to-digital converter (Power1401, Cambridge Electronic Design).

In other experiments, a second glass electrode was used for extracellular single cell and LFP recording in the mPFC. At the end of the recordings, the cells were juxtacellularly labeled (Pinault, 1996) by applying positive current steps with a 200 ms duty cycle. Signals from glass electrodes were amplified (1000×) and bandpass filtered for LFP (0.3–300 Hz) and units (800–5000 Hz) (BF-48DGX and DPA-2FS, NPI Electronic). A Hum-Bug (Digitimer Ltd.) was used to eliminate 50 Hz noise from the LFP signals without distorting phase. The LFP and units were sampled online at 1000 Hz and 20 kHz, respectively (Power1401, Cambridge Electronic Design). All data were collected and analyzed with Spike 2 (Cambridge Electronic Design).

Additionally, in three rats, the LFP in the CA1 area of the dorsal hippocampus was simultaneously recorded with unit activity and LFP in the intermediate CA1, ventral CA1, or ventral subiculum (coordinates relative to bregma: anteroposterior, −6.2 to −8.2 mm; mediolateral, −5.5 mm; dorsoventral, 2.4–5.5 mm) (Paxinos and Watson, 2007) using a glass electrode and an octrode, respectively. Before recording, the octrode tip was covered with 1,1′-dioctadecyl-6,6′-di-(4-sulfophenyl)-3,3,3′, 3′-tetramethylindocarbocyanine (DiI) (Molecular Probes/Invitrogen) for *post hoc* verification of the tetrode position. After one recording session the octrode was lowered ~100 μm to record an additional set of neurons.

Tissue processing and anatomical analysis. After tetrode recording or 1–3 h after juxtacellular labeling, rats were perfused with saline followed by 20 min fixation with 4% paraformaldehyde, 15% (v/v) saturated picrinic acid, and 0.05% glutaraldehyde. Serial coronal sections of the frontal cortex were cut (thickness: 70 μm).

Labeled cells were visualized by immunofluorescence reaction (Streptavidin-Alexa 488, Molecular Probes/Invitrogen), and interneurons were further tested for their molecular expression patterns, including parvalbumin (PV), calbindin (CB), cholecystokinin (CCK), somatostatin (SOM), vasointestinal polypeptide (VIP), and glutamic acid decarboxylase (GAD). Antibodies, with their specification and characterization, are listed in supplemental Table 1, available at www.jneurosci.org as supplemental material.

Sections were converted for light and electron microscopy using an avidin-biotinylated horseradish peroxidase method, incubated in 1–2% osmium tetroxide, and embedded in resin. The areas and layers of the mPFC were differentiated by light microscopy (Gabbott et al., 1997). The somatodendritic and axonal arborizations of labeled cells were determined by light microscopy, and two cells were reconstructed using the Neurolucida system (MicroBrightField) with a 100× oil-immersion objective.

Using electron microscopy, we identified randomly sampled synapses from seven labeled interneurons and determined their postsynaptic targets based on classic criteria (Peters and Palay, 1991).

The recording sites of the tetrodes were verified by light microscopy, for recordings in the mPFC, confirming sites in the PL cortex layers II–V and for recordings in the hippocampus, the pyramidal layer of the intermediate and ventral CA1 area or the ventral subiculum.

Spike sorting. Spikes from tetrode/octrode recordings were extracted from the wide-band signal (Csicsvari et al., 1998). Wide-band signals were bandpass filtered (0.8–5 kHz) and the power (root mean square) was calculated in a 0.2 ms window. All spikes with a power above the threshold (>5 times the SD) were detected. The separation of extracted spikes was based on spike amplitude and wave shapes by using the automatic clustering program KlustaKwik (Harris et al., 2000). Obtained clusters were visualized with Klusters (Hazan et al., 2006), manually separated, merged, and refined according to their feature vectors, waveforms, auto-correlograms, and cross-correlograms to obtain well isolated clusters with a clear refractory period.

Detection of hippocampal theta and prefrontal spindle oscillations. The detection of theta epochs from the CA1 LFP was performed as described previously (Klausberger et al., 2003). The θ (3–6 Hz) to δ (2–3 Hz) frequency power ratio was calculated in a 2 s window. A ratio greater than 4 in three consecutive windows defined a theta period.

In the mPFC, spindle oscillations in the LFP and units were recorded with the same electrode. Spindle oscillations occurred during slow oscillations, which were first detected by calculating the power of the filtered LFP [low-pass 3.5 Hz, Finite Impulse Response (FIR) filter] in a 0.1 s window. Periods with values greater than the mean computed over the complete recording duration were considered further for spindle detection. Spindle oscillations were identified in the filtered LFP (7–14 Hz, FIR-filter) and defined by at least four consecutive cycles (troughs as references) with each cycle duration 0.071–0.125 ms and each cycle amplitude greater than mean +6 SD, computed over the complete recording duration. The start (t_s) and the end (t_e) of a spindle period was extended to $t_s = t_f - ½(t_f - t_{p-1})$ and $t_e = t_l + ½(t_{p+1} - t_l)$ where t_f is the time of the first spindle trough in the period exceeding the detection threshold; t_{p-1} is the time of the spindle peak preceding t_f; t_l is the last trough in the period that exceeds the detection threshold; and t_{p+1} is the time of the spindle peak succeeding t_l.

Analysis of firing patterns during theta and spindle oscillations. Firing patterns of prefrontal cells were analyzed during theta and spindle oscillations. For one interneuron (K64a) no data were recorded during spindle oscillations. When theta oscillations were induced by a pinch, the first 2 s were excluded from the theta analysis because some cells reacted with a higher firing frequency. A prefrontal cell was considered silent, and not included in statistical analysis of firing phase, if the firing frequency during this oscillatory state was ≤0.01 Hz. Troughs of the filtered LFP (3–6 Hz for hippocampal theta oscillations, 7–14 Hz for prefrontal spindle oscillations) were determined, and within a detected theta or spindle period, each spike was assigned to a given phase between the troughs (0° and 360°).

For theta and spindle oscillations, the same analyses were performed to determine the timing relationship of cell firing to the respective cycle phase. Prefrontal cell firing was regarded as significantly modulated when the Rayleigh's test indicated that spike phases were not uniformly distributed around the oscillatory cycle ($p \leq 0.05$) (Zar, 1999). A non-significant result was only accepted if the cell was firing with >0.1 Hz during this oscillation and a minimum number of 25 spikes were detected; otherwise the cell was described as not tested. To compare the average phase distribution between two cell types, a two-sample permutation test (Good, 2000) was applied. The combined mean angle (μ) and mean vector length (r) for each cell type was computed and the difference between the two groups determined. Values for μ and r of each cell were

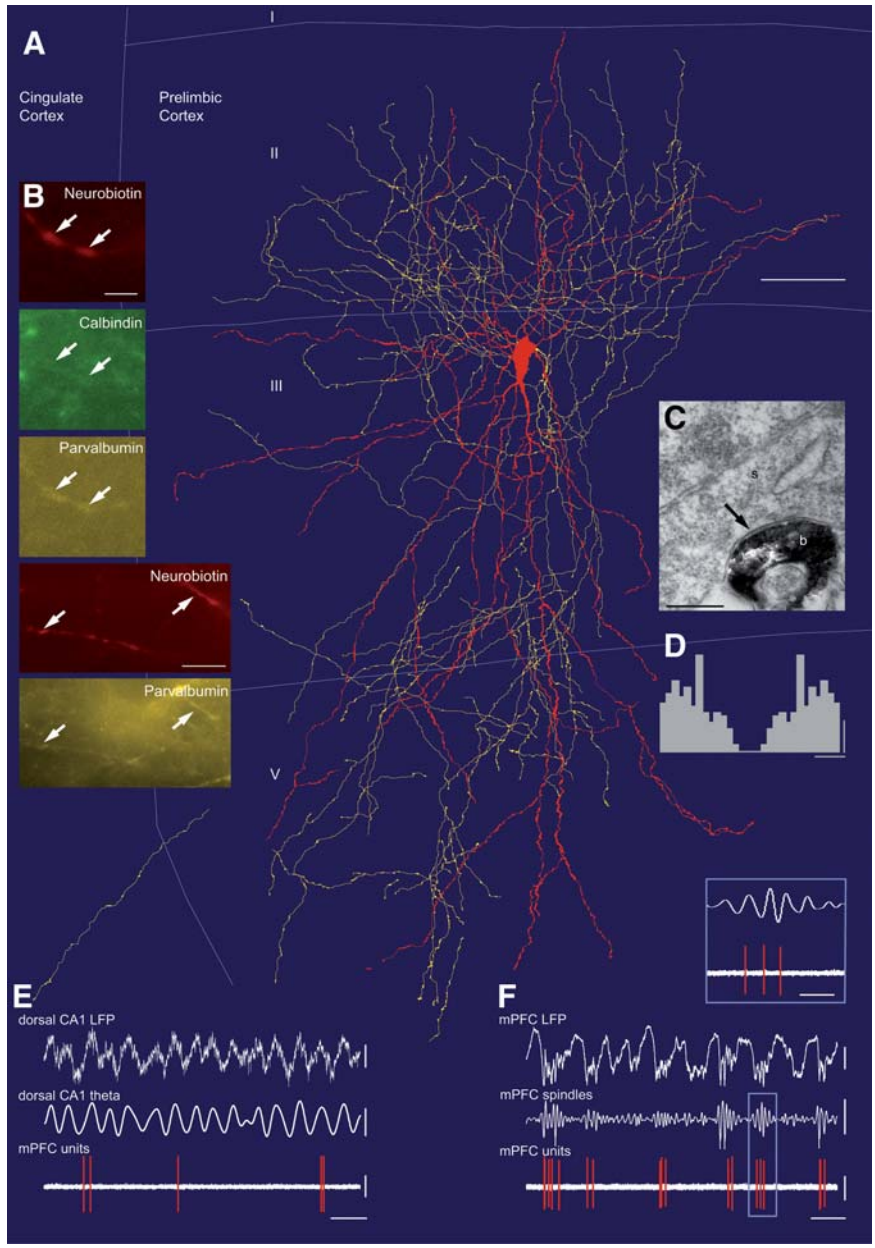

Figure 3. *In vivo* firing patterns of an identified PV+/CB+ basket cell in the prelimbic cortex (K19a) during hippocampal theta and local spindle oscillations. ***A***, Neurolucida reconstruction showing the soma and dendrites in red (completely reconstructed) and axon in yellow (reconstructed from one section, 70 μm thickness). I, II, III, V indicate cortical layers. ***B***, Immunofluorescence micrographs showing neurobiotin-labeled dendrites of this cell; they are immunopositive for parvalbumin and calbindin (arrows). ***C***, Electron micrograph showing a labeled bouton (b) making a type II synapse (arrow) onto a soma (s) of a putative pyramidal cell. ***D***, Autocorrelogram of action potentials. ***E***, Spike timing of the prefrontal cell during theta oscillations recorded extracellularly in the pyramidal cell layer of the dorsal CA1 hippocampus (filtered 3–6 Hz). Note that the cell is firing preferentially at the peak of the oscillations. ***F***, The cell fired at the negative phase of the 1 Hz field oscillations and often at the early ascending phase of the spindle oscillations (inset) recorded extracellularly from the same glass electrode. Note that the cell fired stronger on 1 Hz cycles during which prominent spindle oscillations occurred. Scale bars: ***A***, 50 μm; ***B***, top series, 3 μm; bottom series, 10 μm; ***C***, 0.3 μm. Calibrations: ***D***, 10 spikes and 10 ms; ***E***, CA1 LFP and CA1 theta, 0.3 mV; mPFC units, 1 mV and 0.5 s; ***F***, mPFC LFP, 0.5 mV; mPFC spindles, 0.3 mV; mPFC units, 1 mV and 1 s; inset, 200 ms.

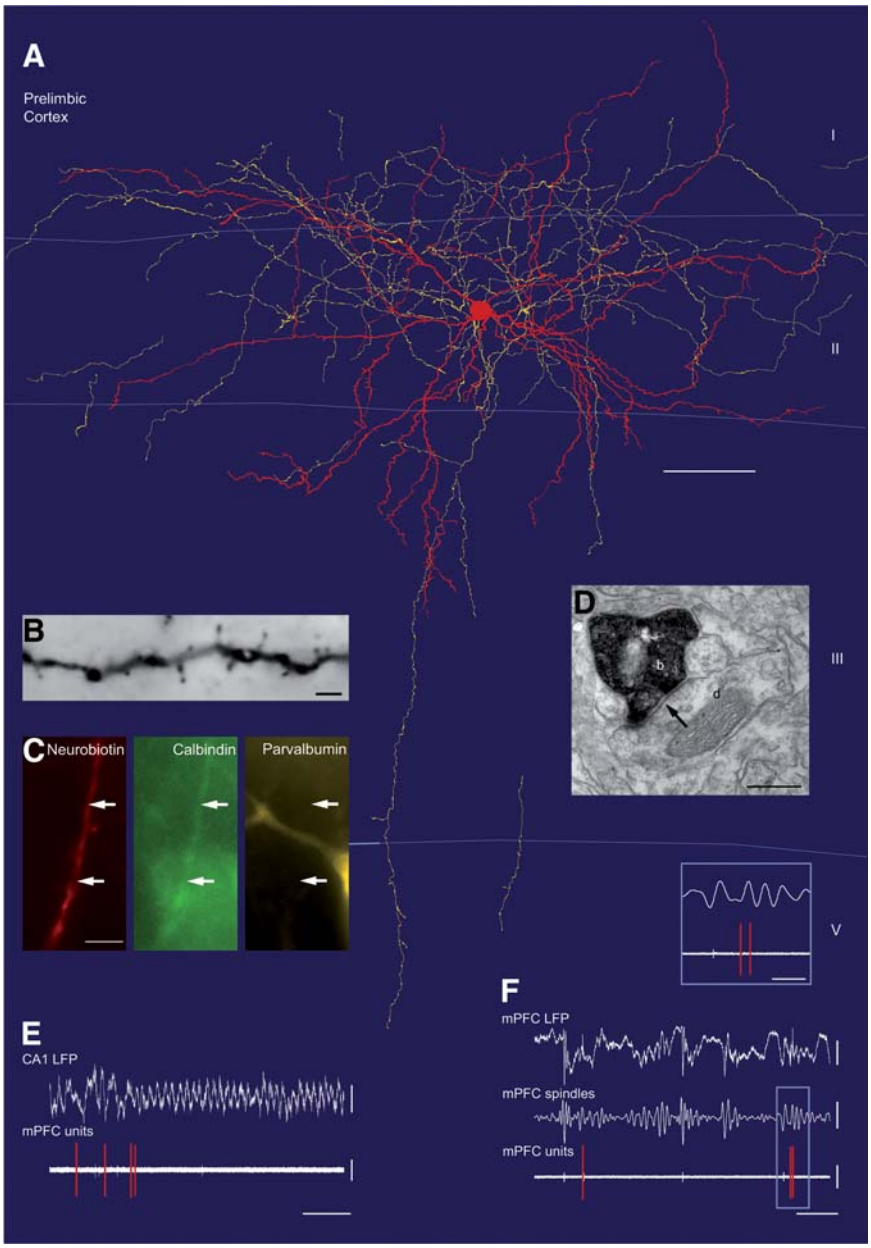

Figure 4. *In vivo* firing patterns of a CB+/PV− dendrite-targeting cell in the prelimbic cortex (K125a) during hippocampal theta and local spindle oscillations. ***A***, Neurolucida reconstruction showing the soma and dendrites in red (completely reconstructed) and axon in yellow (reconstructed from one section, 70 μm thickness). Note that the axon enters layer I, unlike that of basket cells. ***B***, Light micrograph of a medium spiny dendrite of the cell after DAB reaction for neurobiotin. ***C***, Immunofluorescence micrographs showing a neurobiotin-labeled dendrite immunopositive for calbindin but negative for parvalbumin (arrows). Note nearby PV-positive cell. ***D***, Electron micrograph showing a labeled bouton (b) making a type II synapse (arrow) onto a small dendrite (d). ***E***, The cell stops firing at the onset of hippocampal theta oscillations. ***F***, The cell fires sparsely at the negative phase of the extracellular 1 Hz oscillations, but it is not modulated according to the spindle oscillations (inset). Scale bars: ***A***, 50 μm; ***B***, 2 μm; ***C***, 5 μm; ***D***, 0.3 μm. Calibrations: ***E***, CA1 LFP, 0.5 mV; mPFC units, 0.5 mV and 2 s; ***F***, mPFC LFP, 0.5 mV; mPFC spindles, 0.3 mV, mPFC units, 1 mV and 1 s; inset, 20 ms.

randomly reassigned to different cell classes and after 10,000 permutations their difference to the original group difference were calculated to obtain an estimated p value. For small group numbers ($n \leq 10$), all possible permutations were calculated.

Analysis of coherency. The coherence (coh) of two LFP signals a and b was calculated to measure their similarity in frequency content during detected theta periods. Calculation was performed with the Spike2 software of Cambridge Electronic Design and based on the following equation:

$$\mathrm{coh}(f) = \frac{|\sum \mathrm{csd}_{ab}(f)|^2}{\sum \mathrm{psd}_a(f) \sum \mathrm{psd}_b(f)},$$

where $\mathrm{psd}_a(f)$ and $\mathrm{psd}_b(f)$ are the autospectral density functions of a and b at the frequency (f) and $\mathrm{csd}_{ab}(f)$ is the cross-spectral density function between a and b.

To estimate the significance of the coherency values, the LFP signals of the mPFC, intermediate CA1 and ventral CA1 were randomly shifted 100 times within 10 s relative to the dorsal CA1 LFP and the respective coherence histograms were computed. The 95th highest value of each bin from the 100 shuffled histograms was used as the significance threshold for the respective frequency.

Results

Spike timing of putative pyramidal cells in the mPFC of anesthetized rats is synchronized to hippocampal theta oscillations

In freely moving rats, putative pyramidal cells of the mPFC fire rhythmically in relation to theta oscillations in the hippocampus (Hyman et al., 2005; Jones and Wilson, 2005; Siapas et al., 2005; Sirota et al., 2008). To test whether a similar synchronization also occurs in anesthetized rats, we recorded the spike timing of putative pyramidal cells in the PL area of the mPFC with tetrodes and simultaneously detected theta oscillations in the dorsal CA1 area of the hippocampus. Histological analysis confirmed that the recording sites were located in layers II–V of the PL cortex, but the exact laminar position of each unit could not be reliably established. Putative pyramidal cells were selected on the basis that they occasionally fire complex-spike bursts of two to seven spikes at high frequencies (Ranck, 1973), which are highlighted by peaks in the autocorrelograms at 3–10 ms followed by a fast exponential decay (Fig. 1*A*). Of 63 clustered units from 10 tetrode recording sites in two rats, we selected 28 putative pyramidal cells firing in bursts with the criterion that in the autocorrelogram the decay to 75% of the peak value was shorter than 30 ms. Neurons selected with this criterion also matched other physiological criteria typical for putative pyramidal cells (Csicsvari et al., 1998, 1999; Barthó et al., 2004) including broad spike width (0.79 ± 0.44 ms; defined as the width of the unfiltered waveform at 25% of the spike amplitude maximum relative to baseline from the channel of the largest spike amplitude) and generally low firing frequency (1.6 ± 1.4 Hz), although this varied according to the brain state. The units not included in this analysis ($n = 35$) were putative interneurons and possibly pyramidal cells that did not fire in bursts.

The firing of 20 (of 28) putative pyramidal cells in the mPFC were modulated in time according to theta oscillations recorded in the hippocampus. Most cells fired preferentially around the peak of hippocampal theta oscillations detected extracellularly in

the dorsal CA1 pyramidal cell layer (Fig. 1*B*,*D*), on average at 182°, where 0° and 360° mark the troughs of theta oscillations recorded extracellularly in the CA1 pyramidal cell layer. To confirm this observation, we also recorded and juxtacellularly labeled pyramidal cells in layers II and III of the PL cortex with glass electrodes (Fig. 1*E*,*F*). Four of six identified pyramidal cells were modulated in time according to theta oscillations in the dorsal CA1 hippocampus; most of them fired preferentially at the hippocampal theta peak similar to putative pyramidal cells recorded with tetrodes (see Fig. 6*B*). The larger proportion of phase-modulated pyramidal cells compared with previously reported experiments in freely moving rats (Sirota et al., 2008) might be the result of a more stereotyped synchronization of theta oscillations under anesthesia, or different recording sites in different cortical layers or prefrontal subfields, or a different discrimination between putative pyramidal cells and interneurons.

The power spectra calculated from the LFPs in the prefrontal cortex during theta oscillations detected in the dorsal CA1 hippocampus indicated the occurrence of some 4 Hz oscillations in the prefrontal cortex (supplemental Fig. 1, available at www.jneurosci.org as supplemental material). However, the predominant frequency in the prefrontal cortex was ~2 Hz during theta oscillations detected in the dorsal CA1 hippocampus. The coherence coefficient was highest at ~4 Hz between the two areas (supplemental Fig. 1, available at www.jneurosci.org as supplemental material), confirming a synchronization in the theta band. Theta troughs detected in the PL cortex were phase coupled to dorsal CA1 theta oscillations and occurred slightly phase shifted (supplemental Fig. 2, available at www.jneurosci.org as supplemental material).

Overall, our results indicated a synchronization of cellular activity in the theta frequency band between the hippocampus and mPFC in anesthetized rats.

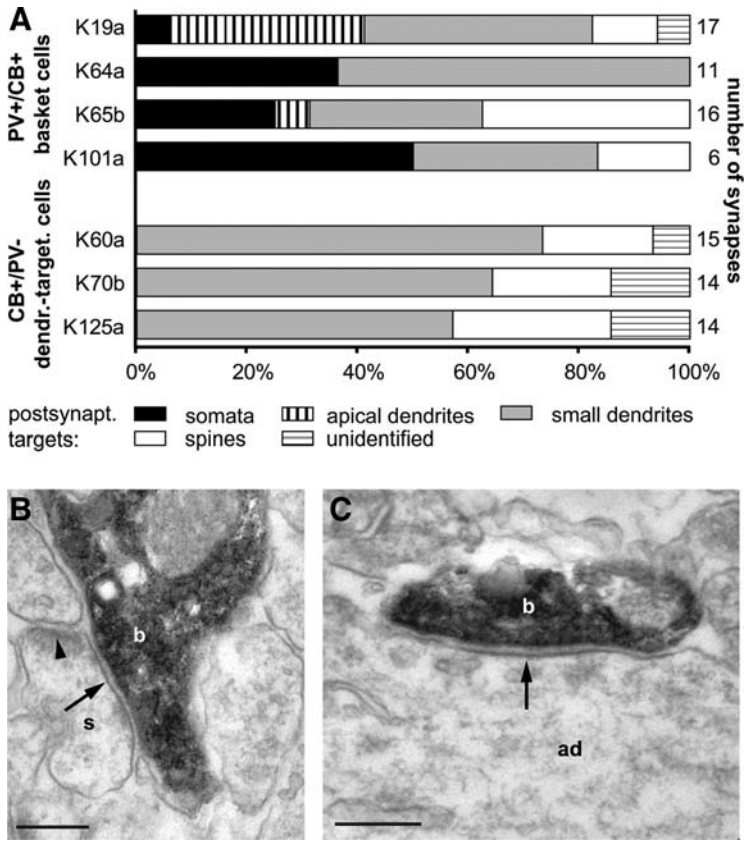

Figure 5. Postsynaptic targets of PV+/CB+ basket cells and CB+/PV− dendrite-targeting cells identified by electron microscopy. ***A***, Randomly sampled synapses from four PV+/CB+ basket cells and three CB+/PV− dendrite-targeting cells (dendr.-target.) demonstrated a distinct postsynaptic (postsynapt.) target preference of the two cell types. ***B***, Electron micrograph showing a labeled bouton (b) from a PV+/CB− basket cell (K19) making a type II synapse (arrow) onto a pyramidal spine (s) also receiving a type I synapse. ***C***, Electron micrograph showing a labeled bouton (b) from the same cell making a type II synapse (arrow) onto an apical dendrite (ad) of a pyramidal cell. Scale bars: 0.2 μm.

Spike timing of putative pyramidal cells in the intermediate and ventral CA1/subiculum relative to the dorsal hippocampal theta cycle

In all experiments, theta oscillations were recorded in the dorsal CA1 area because theta oscillations are highly coherent across this relatively flat structure, and the CA1 pyramidal cell layer could be reliably found as a reference point, allowing comparison between different experiments. Because the monosynaptic input from the hippocampus to the PL cortex arises mainly from the CA1 of the ventral and intermediate hippocampus (Hoover and Vertes, 2007), we recorded and analyzed the phase relationship between pyramidal cells in the intermediate and ventral CA1 (Fig. 2*A*) and theta oscillations in the dorsal CA1 area. We recorded 28 putative pyramidal cells from 10 different and histologically confirmed sites in the ventral CA1 hippocampus from a total of five rats. In addition, we recorded the activity of 36 putative pyramidal cells from six different and histologically confirmed sites in the intermediate CA1 hippocampus from four rats. Putative pyramidal cells were identified based on the same criteria used to select pyramidal cells in the mPFC (see above). Selected hippocampal pyramidal cells were characterized by an average spike width of 0.52 ± 0.17 ms and an average firing frequency of 1.7 ± 1.9 Hz. All pyramidal cells ($n = 64$) were significantly modulated to the dorsal hippocampal theta cycle (Rayleigh's test, $p \leq 0.05$). Pyramidal cells in the intermediate CA1 fired preferentially at the ascending phase of the dorsal theta cycle (Fig. 2*B*) with a mean preferred phase of 63° (Fig. 2*D*). Pyramidal cells in the ventral CA1 area fired later than pyramidal cells of the intermediate area and phase coupled to the peak of the dorsal theta cycle (mean preferred phase: 187°) (Fig. 2*C*, *D*). Dorsal CA1 pyramidal cells have been reported to fire strongest at 20° just after the trough of dorsal CA1 theta oscillations under similar conditions (Klausberger et al., 2003) and also in drug-free rats (Skaggs et al., 1996). In two animals, intermediate and ventral CA1 pyramidal cells were recorded consecutively and without moving the dorsal CA1 reference electrode. In both experiments the intermediate CA1 pyramidal cells fired significantly earlier during dorsal CA1 theta compared with the spike timing of the ventral CA1 pyramidal cells ($p = 0.02$, $n = 18$ and $p < 0.01$, $n = 20$; permutation test). Therefore, our data indicate a gradual shift of CA1 pyramidal cells firing relative to dorsal CA1 theta oscillations along the dorsoventral axis. Because ventral CA1 pyramidal cells provide a

Table 1. Molecular expression profile, discharge frequency, and mean firing angles during theta and spindle oscillations of identified PV+/CB + basket cells and CB+/PV− dendrite-targeting cells

	Molecular expression						Theta oscillations		Spindle oscillations	
	PV	CB	GAD	CCK	SOM	VIP	f-freq.	m. angle ± SD; *p*	f-freq.	m. angle ± SD; *p*
PV+/CB+ basket cells										
K19a	+	+¹			−		0.2 Hz	198 ± 81°; 0.002	4.1 Hz	47 ± 122°; <0.001
K64a	+						3.2 Hz	176 ± 60°; 0.006		
K65b	+	+					0.1 Hz	145 ± 78°; <0.001	0.5 Hz	36 ± 99°; 0.002
K94e	+	+¹					0.8 Hz	156 ± 65°; <0.001	17.1 Hz	36 ± 57°; <0.001
K101a	+	+¹					0.2 Hz	202 ± 77°; <0.001	9.3 Hz	42 ± 120°; 0.001
K124a	+	+¹					5.9 Hz	143 ± 59°; <0.001	7.3 Hz	34 ± 48°; <0.001
K126c	+	+¹					0.01 Hz		5.5 Hz	83 ± 79°; <0.001
K142a	+	+					0 Hz		2.7 Hz	314 ± 70°; <0.001
K145a	+	+	+				0 Hz		0.7 Hz	n.s.
K148c	+						1 Hz	164 ± 4°; <0.001	9.2 Hz	0 ± 79°; <0.001
CB+/PV− dendrite-targeting cells										
K60a	−	+		−			0.1 Hz	n.s.	4.4 Hz	n.s.
K70b	−	+	+	−	−		0.1 Hz	n.s.	1.3 Hz	n.s.
K125a	−	+	+	−	−	−	0.05 Hz		1 Hz	n.s.

Significance of mean firing phase was only determined for cells firing at least 0.1 Hz.

+, Immunopositive; +¹, immunoreactivity was judged weakly positive by comparing the labeling to other nonlabeled cells in the same field; −, immunonegative; f-freq, firing frequency; m. angle, mean angle; n.s., not significant; *p*, *p* value for Rayleigh's test.

major monosynaptic input to the prefrontal cortex and because these cells fire at a similar theta phase compared with prefrontal pyramidal cells, the ventral CA1 might drive the neuronal activity in the prefrontal cortex during theta oscillations.

The power and coherence spectra (supplemental Fig. 1, available at www.jneurosci.org as supplemental material) calculated from the LFPs in the intermediate hippocampus during theta oscillations detected in the dorsal CA1 hippocampus indicated a strong 4 Hz theta oscillation in the intermediate hippocampus that was highly coherent with dorsal CA1 theta. In the ventral hippocampus, a 4 Hz oscillation coherent to dorsal CA1 theta was present, but the predominant frequency in the ventral hippocampus was ~2 Hz during theta oscillations detected in the dorsal CA1 hippocampus. Theta troughs detected in the intermediate CA1 occurred at the ascending phase of dorsal CA1 theta oscillations (supplemental Fig. 2, available at www.jneurosci.org as supplemental material). Theta troughs detected in the ventral CA1 hippocampus from individual recordings were phase coupled to the dorsal CA1 theta cycles. However, the phase relation of ventral CA1 theta troughs to dorsal CA1 theta oscillations varied strongly between different recording sites. Interestingly, putative pyramidal cells in the ventral CA1 area were phase coupled to the peak of dorsal CA1 theta oscillations regardless of the recording site. This suggests that field theta oscillations in the ventral CA1 hippocampus might be strongly influenced by volume conduction attributable to its own curvature and the geometry of the surrounding structures, which may also oscillate at theta frequency. Alternatively, the reversal of theta oscillations might occur close to or within the pyramidal cell layer in the ventral hippocampus.

Distinct molecular expression profile and postsynaptic targets of basket and dendrite-targeting cells in the prelimbic cortex

GABAergic interneurons make a key contribution to generate theta oscillations in the hippocampus (Somogyi and Klausberger, 2005; Klausberger and Somogyi, 2008). To test whether different types of prefrontal interneurons participate in the synchronization of prefrontal pyramidal cells to hippocampal theta oscillations, we recorded the spike timing of single interneurons in the PL cortex during hippocampal theta oscillations using glass electrodes. Subsequently, we filled the recorded neurons with neurobiotin using the juxtacellular labeling method (Pinault, 1996; Klausberger et al., 2003) and determined their dendritic and axonal arborization, postsynaptic targets, and expression of calcium-binding proteins (Figs. 3, 4). This analysis revealed 10 PV+/CB+ basket cells and three CB+/PV− dendrite-targeting cells in layer II or III of the PL cortex. In one case, the laminar position of the cell was estimated by its proximal dendrites and axon, because the soma could not be recovered.

The somata of the basket cells were round or oval shaped and located in layers II ($n = 5$) and III ($n = 5$). The position of the soma did not result in differences in their dendritic or axonal distribution and firing patterns. Cells had smooth, multipolar dendrites, which were mostly radially oriented and covered PL cortex layer II to layer V. The characteristically dense axonal arborization was mostly concentrated in lower layer II/upper layer III and lower layer III/upper layer V (Fig. 3*A*). Axons did not cross the border to layer I, where dendritic tufts of pyramidal cells are located. In addition, only sparse axon was observed in neighboring areas (cingulate cortex, medial orbital cortex and infralimbic cortex). Light microscopic evaluation indicated that the axon of these cells preferentially targeted the somata and proximal dendrites of pyramidal cells. To confirm this observation, four (of 10) cells showing basket-like axonal arbors were randomly selected and their postsynaptic targets were tested by electron microscopy (Figs. 4*C*, 5*A*). Randomly sampled synapses ($n = 50$) from the labeled cells were confirmed as type II synapses and they targeted somata (29 ± 19%), apical dendrites (10 ± 17%), small dendrites (42 ± 15%), and spines (16 ± 16%); 1 ± 3% of the postsynaptic targets remained unidentified, because they could have been either spines or small dendrites. The majority of the postsynaptic targets are expected to originate from pyramidal cells but clear criteria for discriminating pyramidal cells and interneurons could not be found in this neocortical area. Overall, the electron microscopic analysis confirmed the identity of light microscopically predicted basket cells.

Using immunofluorescence microscopy (Fig. 3*B*, Table 1), the dendrites and/or somata of all labeled basket cells ($n = 10$) were immunopositive for PV. In addition, eight of the cells could be

tested for immunoreactivity for CB and all eight cells were immunopositive, although the immunoreactivity for CB varied from cell to cell and could be very low compared with adjacent CB-positive cells in the same area. In some cases the signal could only be detected in the labeled soma, but not in proximal dendrites and was judged weakly positive (Table 1; supplemental Fig. 3, available at www.jneurosci.org as supplemental material). A possible cross-reactivity of the calbindin antibody for PV could be excluded because of the lack of CB immunoreactivity of PV-positive interneurons in the pyramidal cell layer of the hippocampus. The axon of one of the basket cells was also tested for GAD, and shown to be immunopositive confirming the classification of the cell as a GABAergic interneuron.

The three dendrite-targeting interneurons had profusely branching axons in layer II, also spreading into layer I, overlapping with dendritic apical tufts of pyramidal cells (Fig. 4*A*); only few axonal branches reached deeper layers. The somata were located in layer II and the dendrites branched mainly in layer II but reached also into layer I and upper layer III. The dendrites of two of the cells emitted significant numbers of spines (Fig. 4*A*,*B*). Electron microscopic analysis revealed that the three cells innervated small dendritic shafts (65 ± 8%) and spines (23 ± 5%) with type II synapses (12 ± 4% of the targets were unidentified, because they could have been either spines or small dendrites), but avoided somata and main apical dendrites (Fig. 5*A*) in contrast to basket cells.

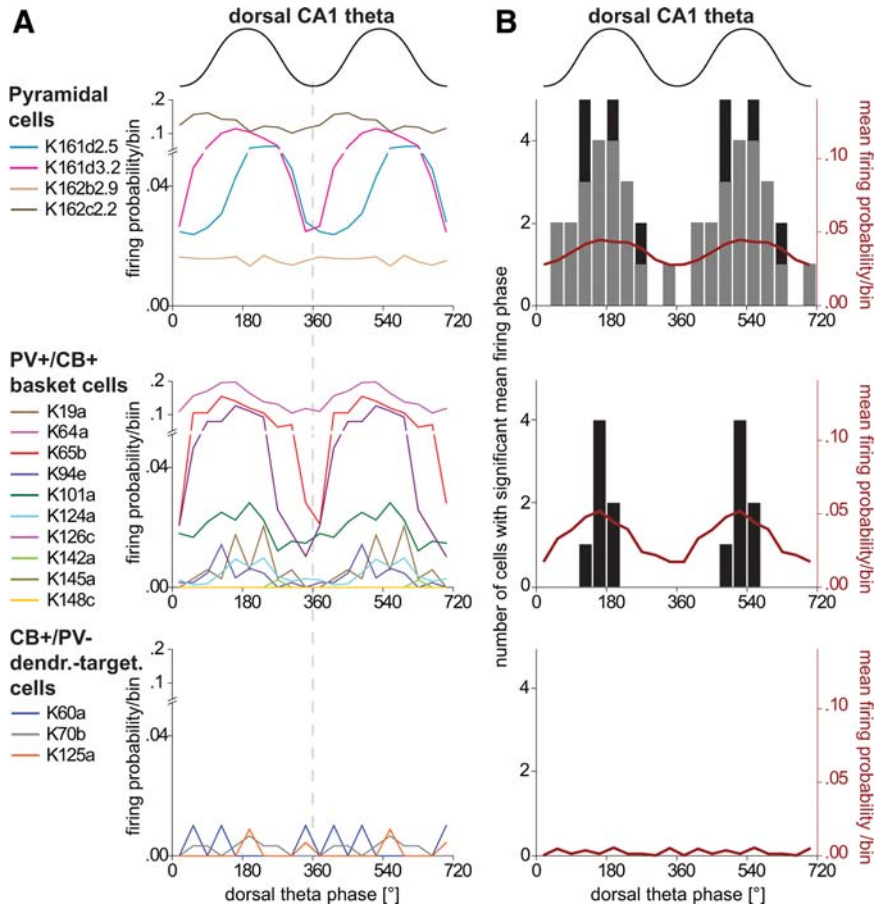

Figure 6. Comparison of the spike timing of putative and identified pyramidal cells, identified PV+/CB+ basket cells, and identified CB+/PV− dendrite-targeting cells in the prefrontal cortex during theta oscillations recorded extracellularly in the pyramidal cell layer of the dorsal CA1 hippocampus. ***A***, ***B***, Upper schematic waveform indicates two dorsal CA1 theta cycles; 0° and 360° mark the troughs. ***A***, Firing probability of individual cells (colored traces) within a theta cycle (bin size 36°). Only four examples of putative pyramidal cells are shown for clarity. ***B***, The columns and left *y*-axis indicate the number of cells observed with a significant mean firing phase. Black columns represent identified and juxtacellularly labeled cells and gray columns represent putative pyramidal cells recorded with tetrodes. The red curve and right *y*-axis indicate the mean firing probability of all cells from a particular type. Note that pyramidal cells and PV+/CB+ basket cells have similar mean firing probabilities at the peak of the theta cycle; none of the CB+/PV− dendrite-targeting cells were significantly modulated. dendr.-target., Dendrite-targeting.

Using immunofluorescence analysis, the axons of two dendrite-targeting cells were tested for GAD; their immunopositivity confirmed their identity as GABAergic interneurons (Table 1). The dendrites of all three dendrite-targeting cells were strongly immunopositive for CB compared with other immunopositive nonlabeled cells in the same area. Contrary to PV+/CB+ basket cells, all dendrite-targeting cells were immunonegative for PV, as tested on their dendrites. All three dendrite-targeting cells were also immunonegative for CCK (two cells were tested on the soma, one cell on the axon). The somata of two cells were tested for their expression of SOM and both were immunonegative, and the soma of one neuron was tested and negative for VIP (Table 1).

Firing patterns of pyramidal cells, PV+/CB+ basket cells, and CB+/PV− dendrite-targeting cells during theta oscillations in the dorsal hippocampus

To test whether PV+/CB+ basket and CB+/PV− dendrite-targeting cells fire rhythmically and make different contributions to the synchronization of the PL area to hippocampal theta oscillations, we quantitatively analyzed the firing patterns of these interneurons and compared them with the firing of putative pyramidal cells in the PL area.

During theta oscillations, prefrontal pyramidal cells fired with an average rate of 1.4 ± 1.5 Hz, which was in the same range as the average firing rate of PV+/CB+ basket cells (1.1 ± 2.0 Hz). Three (of 10) basket cells fired with <0.1 Hz during theta oscillations (Table 1). The firing rate of all CB+/PV− dendrite-targeting cells dropped dramatically when the hippocampal LFP changed from slow oscillations to theta oscillations (Fig. 4*E*, Table 1), and they were generally silent during theta (0.08 ± 0.03 Hz).

The majority of prefrontal pyramidal cells (24 of 34) fired phase modulated during hippocampal theta oscillations (Rayleigh's test, $p \leq 0.05$). Modulated pyramidal cells fired often around the peak of hippocampal theta oscillations, but individual cells showed a broad range of preferred phases (Fig. 6*B*), their distribution clearly centered at the peak of the theta cycle (overall mean firing phase $\mu = 177°$; overall mean firing vector length $r = 0.14$; 0° and 360° mark the troughs of theta oscillations recorded extracellularly in the dorsal CA1 pyramidal cell layer). All PV+/CB+ basket cells that fired with ≥0.1 Hz during theta oscillations (7 of 10) were also significantly phase coupled to hippocampal theta waves (Rayleigh's test, $p \leq 0.05$). Modulated PV+/CB+ basket cells fired also preferentially around the peak of hippocampal theta oscillations ($\mu = 173°$) (Fig. 6), which is similar

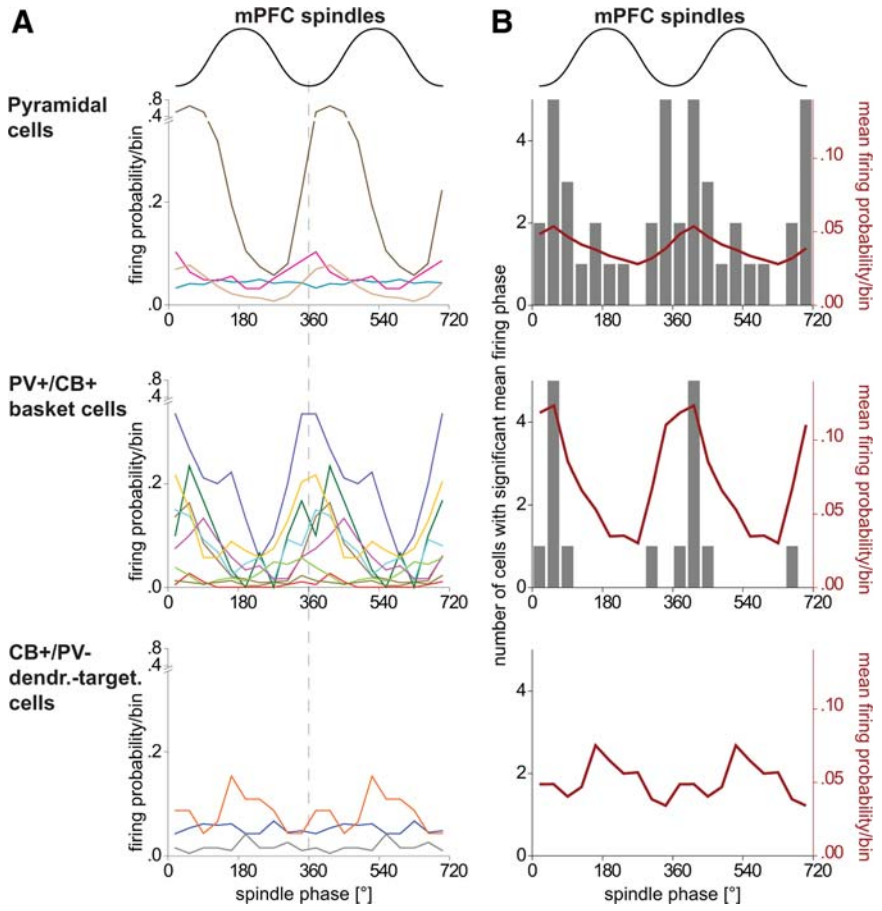

Figure 7. Comparison of the spike timing of putative pyramidal cells, identified PV+/CB+ basket cells and identified CB+/PV− dendrite-targeting cells during prefrontal spindle oscillations. ***A***, ***B***, Upper schematic waveform indicates two mPFC spindle cycles; 0° and 360° mark the troughs. ***A***, Firing probability of individual cells (colored traces, same cells and color code as in Fig. 6) during a spindle cycle (bin size 36°). Only four examples of pyramidal cells are shown for clarity. ***B***, The gray columns and left *y*-axis indicate the number of cells observed with a significant mean firing phase. The red curve and right *y*-axis indicate the mean firing probability of all significantly modulated cells. Note that PV+/CB+ basket cells discharge at a phase similar to that of pyramidal cells; none of the CB+/PV− dendrite-targeting cells were significantly modulated during spindle oscillations. dendr.-target., Dendrite-tageting.

to the mean firing angles of pyramidal cells (two-sample permutation test, $p = 0.85$, $n = 31$). The distribution of mean firing phases of individual PV+/CB+ basket cells was more concentrated compared with pyramidal cells, which was also indicated by a significantly larger r value ($r = 0.36$, two-sample permutation test, $n = 24$, p~0.007). In contrast to the basket and pyramidal cells, the few spikes recorded of the CB+/PV− dendrite-targeting cells during theta oscillations did not occur on a preferred theta phase (Rayleigh's test, $p > 0.1$). Overall, these results indicate that PV+/CB+ basket cells contribute to the synchronization of theta oscillations between the hippocampus and prefrontal cortex and fire at the same time as prefrontal pyramidal cells. In contrast, CB+/PV− dendrite-targeting cells of the PL cortex stop firing during hippocampal theta oscillations.

Firing patterns of pyramidal cells, PV+/CB+ basket cells, and CB+/PV− dendrite-targeting cells during prefrontal spindle oscillations

In addition to theta oscillations, the firing patterns of prefrontal pyramidal, PV+/CB+ basket, and CB+/PV− dendrite-targeting cells were also recorded during locally detected spindle oscillations. Spindle oscillations (7–14 Hz), recorded in the mPFC, were always organized by slow oscillations, characterized by alternating up and down states at low frequency (~1 Hz), and large amplitude. Spindles occurred always on the intracellular up state of the slow oscillations, which is indicated by the negative phase of the LFP (Figs. 1*C*, 3*F*, 4*F*). The LFP recorded simultaneously in the CA1 area of the dorsal hippocampus was characterized by large-amplitude slow oscillations (Fig. 1*C*).

During spindle oscillations, PV+/CB+ basket cells ($n = 9$), putative pyramidal cells recorded with tetrodes ($n = 28$), and CB+/PV− dendrite-targeting cells ($n = 3$) fired with 6.3 ± 5.2 Hz, 3.4 ± 4.6 Hz, and 2.2 ± 1.9 Hz, respectively (Table 1). Because juxtacellulalry labeled pyramidal cells were recorded mainly during theta oscillations and only few data could be obtained during spindle oscillations, these cells were not included in this analysis. The majority of putative pyramidal cells (22 of 28) and PV+/CB+ basket cells (8 of 9) were significantly phase coupled to local spindle oscillations (Rayleigh's test, $p \leq 0.05$) (Fig. 7). Pyramidal cells fired around the trough of extracellular spindle cycles ($\mu = 7.5°$; $r = 0.1$) (Figs. 1*C*,*D*, 7) and PV+/CB+ basket cells fired at the trough and early ascending phase of the local spindle oscillations ($\mu = 32.5°$; $r = 0.36$) (Figs. 3*F*, 7). The firing phase between pyramidal and basket cells was not significantly different (permutation test, $n = 30$, $p = 0.45$), but phase locking (r) was stronger for basket cells (permutation test, $n = 30$, $p = 0.004$). In contrast to pyramidal and basket cells, none of the CB+/PV− dendrite-targeting cells fired phase modulated according to local spindle oscillations (Rayleigh's test, $p > 0.05$), although these cells had firing frequencies comparable to those of pyramidal cells (Figs. 4*F*, 7). Overall, these results indicate that spindle oscillations are coupled with a high firing rate and phase locking of PV+/CB+ basket cells, but CB+/PV− dendrite-targeting cells do not contribute to the synchronizing pyramidal cells during spindle oscillations.

Discussion

We have shown that two distinct types of prefrontal cortical interneurons, defined by their axonal and dendritic arborization, synaptic connectivity, and molecular expression patterns, have different spike timing during hippocampal theta and local spindle oscillations *in vivo*. Because pyramidal cell firing is also modulated by these network patterns, our data suggest that basket cells modulate theta and spindle oscillation-related synchronization on the perisomatic domain, whereas dendrite-innervating calbindin-expressing interneurons do not contribute to field oscillations.

Prefrontal PV+/CB+ basket and pyramidal cell firing *in vivo*

The basket cells recorded and labeled in this study had typical multipolar, smooth dendrites with dense axonal arborization making synaptic contacts onto somata and proximal dendrites, which distinguishes them from previously described

parvalbumin-expressing, multipolar bursting interneurons, which mainly innervate dendrites and spines (Blatow et al., 2003). The coexpression of PV and CB by basket cells has been described before in the neocortex (Cauli et al., 1997; Kawaguchi and Kubota, 1997; Markram et al., 2004), which is different in the CA1 area of the hippocampus, where PV-expressing basket cells are CB immunonegative.

We found that most prefrontal PV+/CB+ basket cells fired rhythmically in relation to hippocampal theta and local spindle oscillations. Interestingly, modulated PV+/CB+ basket cells were tightly coupled to the same theta and spindle phase as modulated prefrontal pyramidal cells. This finding suggests that synchronized activity, generated in the hippocampal formation (Buzsaki, 2002) or the thalamus (Steriade et al., 1985, 1987), activates prefrontal pyramidal cells and PV+/CB+ basket cells simultaneously. Therefore, PV+/CB+ basket cells do not generate intracellular theta oscillations in pyramidal cells by hyperpolarizing them in counter phase to their firing, but instead modulate the firing of pyramidal cells when they are most depolarized. Our results support the idea that synaptic integration depends on the precise spatial and temporal characteristics of synaptic inputs changing with the state of the cortical network (Destexhe and Paré, 1999; Hô and Destexhe, 2000; Azouz, 2005). Axons of PV+/CB+ basket cells innervate the somatodendritic domains of pyramidal cells and exert strong influence on the summation of synaptic and intrinsic voltage-gated conductances. Firing of PV+/CB+ basket cells, rhythmically activated by hippocampal or thalamic input at the same oscillatory phase as pyramidal cells, might lead to an increase in the $GABA_A$ receptor-mediated conductance of pyramidal cells with small or no effect on the membrane potential. Consequently, only pyramidal cells receiving strong excitatory inputs might be activated (Koch and Segev, 2000), resulting in a sparse coding of information in the prefrontal cortex during theta oscillations. In addition to regulating the firing rate of pyramidal cells, the firing of PV+/CB+ basket cells shortens the integration window for excitation by providing a feedforward inhibition (Buzsaki, 1984; Gabernet et al., 2005) leading to synchronous firing of pyramidal cells on a millisecond time scale and the formation of cell assemblies (Azouz, 2005).

The relatively small power and amplitude of theta oscillations in the LFP of the prefrontal cortex compared with those in the hippocampus might be explained by the simultaneous firing of PV+/CB+ basket and pyramidal cells, as opposed to different firing phases in the CA1 hippocampus. However, it remains to be investigated whether other interneurons innervating the perisomatic domain of pyramidal cells, such as axo-axonic and CCK-expressing interneurons, might provide differently timed GABAergic input during theta oscillations. Distinct GABAergic interneurons have been described to differentially modulate pyramidal cells and cell assemblies *in vitro* (Szabadics et al., 2007; Molnár et al., 2008). Recently, two populations of fast spiking interneuron, including PV-positive basket cells, were reported with different firing patterns in the frontal cortex *in vivo* (Puig et al., 2008). So-called "early fast spiking interneurons" were strongly coupled to the spindle cycle and fired during earlier phases than "late firing fast spiking cells". During desynchronized prefrontal states, when hippocampal theta might increase (not recorded in the above study), early fast spiking cells decreased and late spiking cells increased their activity. We found that three identified PV+/CB+ basket cells in our sample were silent during hippocampal theta oscillations, but these cells showed no difference in their strength of coupling to the spindle cycle or preferred phase compared with theta-active PV+/CB+ basket cells.

Spindle and theta oscillations observed under anesthesia in our experiments occurred spontaneously (Clement et al., 2008). However, a possible effect of the anesthesia on the firing rate and patterns of prefrontal neurons cannot be excluded.

Neurons in the mPFC might be driven by monosynaptic inputs form ventral hippocampus during theta oscillations

Anatomical studies revealed that pyramidal cells and PV+ basket cells in the mPFC receive monosynaptic input from the ventral CA1 and subiculum (Swanson, 1981; Jay and Witter, 1991; Gabbott et al., 2002). We have shown that pyramidal cells of the ventral hippocampus fire with their highest probability at the peak of the dorsal CA1 theta cycle. Interestingly, this is the same theta phase when pyramidal cells and PV+/CB+ basket cells in the PL area of the mPFC are firing most. Previously it has been reported that single pulse stimulation in the hippocampus induced an early EPSP of fixed latency (14.6 $\pm$ 4.0 ms) in most prefrontal pyramidal cells (Dégenètais et al., 2003) and short-latency excitatory response (16.3 $\pm$ 4.1 ms) in identified interneurons (Tierney et al., 2004), typical for monosynaptic hippocampal-prefrontal connections (Ferino et al., 1987). This time delay is consistent with the small difference in theta phase firing of ventral hippocampal and prefrontal neurons and supports a monosynaptic prefrontal activation from the ventral CA1 area during theta oscillations.

The dorsal hippocampus is preferentially involved in spatial memory (Moser and Moser, 1998), whereas the contributions of the ventral hippocampus seem to be different, but are less clear. Dorsal CA1 pyramidal cells have smaller place fields, and higher mean and peak firing rates (Maurer et al., 2005), a larger proportion of dorsal CA1 pyramidal cells have place fields (Jung et al., 1994), and lesion of the ventral hippocampus does not affect basic spatial behaviors (Bannerman et al., 2002). Therefore, it appears to be necessary that information not only from the ventral but also from the dorsal hippocampus be conveyed to the prefrontal cortex. However, monosynaptic connections are rare from the dorsal hippocampus to the prefrontal cortex. In addition, during ongoing hippocampal theta oscillations under anesthesia, pyramidal cells in the dorsal CA1 area fire preferentially around the trough of the theta cycle (Klausberger et al., 2003), whereas prefrontal neurons fired most at the peak, which is not consistent with a monosynaptic activation. Interestingly, the phase locking of prefrontal and hippocampal pyramidal cells to the theta peak and trough, respectively, has also been reported in freely moving rats, in which theta oscillations occur at a significantly faster frequency of 6–10 Hz (Hyman et al., 2005; Siapas et al., 2005). The preservation of spike timing relative to theta phase, rather than absolute time, suggests that dorsal hippocampal–prefrontal communication is governed by conduction delays (Lubenov and Siapas, 2008) and intermediate structures, which correlate the incoming inputs to local activities and theta oscillations and generate distinctly timed cell assemblies rather than monosynaptic mirror images of their inputs. Possible intermediate structures include the subiculum, entorhinal cortex, and thalamus (Hoover and Vertes, 2007). A synchronization of theta oscillations across structures might also be supported by inputs from the basal forebrain and the medial septum (Jones, 2008) and might also be modulated by the dopaminergic system (Kröner et al., 2007; Goto and Grace, 2008; Tierney et al., 2008).

Distinct firing patterns of CB+/PV− dendrite-targeting cells

We recorded and identified three GABAergic interneurons, expressing CB but not PV, with medium spiny dendrites and

axons innervating small dendrites and spines only, and also firing differently from PV+/CB+ interneurons. The CB+/PV− dendrite-targeting cells showed homogenous firing patterns as they were mostly silent during theta oscillations and their sparse firing was not phase modulated to hippocampal theta cycles. This implies that CB+/PV− dendrite-targeting cells are not directly or indirectly activated by hippocampal-prefrontal pathways. Strikingly, during local spindle oscillations, CB+/PV− dendrite-targeting cells were active and fired with a firing frequency similar to that of prefrontal pyramidal cells, but their firing was not phase modulated by the spindle cycles. However, a possible effect of the anesthesia on the firing patterns of these cells cannot be excluded. Only the preferred firing of these cells on the depth negative phase (up state) of the 1 Hz oscillations suggests some involvement in rhythmic network activity. The sources of the synaptic inputs that silence these cells during theta oscillations, and lead to their surprising spike timing during spindle oscillations, remain to be established.

In conclusion, we have demonstrated that two identified types of GABAergic prefrontal interneuron provide differential spatiotemporal input to pyramidal cells depending on the ongoing brain states as defined by hippocampal theta or local spindle oscillations. The temporal interactions of distinct pyramidal cells and interneurons within and between specific networks might explain how cognitive information is processed and how alterations in their connection or spike timing lead to cognitive dysfunctions (Lewis et al., 2005).

References

Ali AB, Thomson AM (2008) Synaptic alpha 5 subunit-containing GABAA receptors mediate IPSPs elicited by dendrite-preferring cells in rat neocortex. Cereb Cortex 18:1260–1271.

Ascoli GA, Alonso-Nanclares L, Anderson SA, Barrionuevo G, Benavides-Piccione R, Burkhalter A, Buzsáki G, Cauli B, Defelipe J, Fairén A, Feldmeyer D, Fishell G, Fregnac Y, Freund TF, Gardner D, Gardner EP, Goldberg JH, Helmstaedter M, Hestrin S, Karube F, et al. [Petilla Interneuron Nomenclature Group] (2008) Petilla terminology: nomenclature of features of GABAergic interneurons of the cerebral cortex. Nat Rev Neurosci 9:557–568.

Azouz R (2005) Dynamic spatiotemporal synaptic integration in cortical neurons: neuronal gain, revisited. J Neurophysiol 94:2785–2796.

Bacci A, Huguenard JR, Prince DA (2005) Modulation of neocortical interneurons: extrinsic influences and exercises in self-control. Trends Neurosci 28:602–610.

Bannerman DM, Deacon RM, Offen S, Friswell J, Grubb M, Rawlins JN (2002) Double dissociation of function within the hippocampus: spatial memory and hyponeophagia. Behav Neurosci 116:884–901.

Barthó P, Hirase H, Monconduit L, Zugaro M, Harris KD, Buzsáki G (2004) Characterization of neocortical principal cells and interneurons by network interactions and extracellular features. J Neurophysiol 92:600–608.

Beaulieu C, Somogyi P (1990) Targets and quantitative distribution of GABAergic synapses in the visual cortex of the cat. Eur J Neurosci 2:296–303.

Blatow M, Rozov A, Katona I, Hormuzdi SG, Meyer AH, Whittington MA, Caputi A, Monyer H (2003) A novel network of multipolar bursting interneurons generates theta frequency oscillations in neocortex. Neuron 38:805–817.

Buzsáki G (1984) Feed-forward inhibition in the hippocampal formation. Prog Neurobiol 22:131–153.

Buzsáki G (2002) Theta oscillations in the hippocampus. Neuron 33:325–340.

Buzsáki G, Draguhn A (2004) Neuronal oscillations in cortical networks. Science 304:1926–1929.

Cauli B, Audinat E, Lambolez B, Angulo MC, Ropert N, Tsuzuki K, Hestrin S, Rossier J (1997) Molecular and physiological diversity of cortical nonpyramidal cells. J Neurosci 17:3894–3906.

Cauli B, Porter JT, Tsuzuki K, Lambolez B, Rossier J, Quenet B, Audinat E (2000) Classification of fusiform neocortical interneurons based on unsupervised clustering. Proc Natl Acad Sci U S A 97:6144–6149.

Cenquizca LA, Swanson LW (2007) Spatial organization of direct hippocampal field CA1 axonal projections to the rest of the cerebral cortex. Brain Res Rev 56:1–26.

Clement EA, Richard A, Thwaites M, Ailon J, Peters S, Dickson CT (2008) Cyclic and sleep-like spontaneous alternations of brain state under urethane anaesthesia. PLoS ONE 3:e2004.

Contreras D, Destexhe A, Sejnowski TJ, Steriade M (1997) Spatiotemporal patterns of spindle oscillations in cortex and thalamus. J Neurosci 17:1179–1196.

Csicsvari J, Hirase H, Czurko A, Buzsáki G (1998) Reliability and state dependence of pyramidal cell-interneuron synapses in the hippocampus: an ensemble approach in the behaving rat. Neuron 21:179–189.

Csicsvari J, Hirase H, Czurkó A, Mamiya A, Buzsáki G (1999) Oscillatory coupling of hippocampal pyramidal cells and interneurons in the behaving rat. J Neurosci 19:274–287.

Dalley JW, Cardinal RN, Robbins TW (2004) Prefrontal executive and cognitive functions in rodents: neural and neurochemical substrates. Neurosci Biobehav Rev 28:771–784.

DeFelipe J (1993) Neocortical neuronal diversity: chemical heterogeneity revealed by colocalization studies of classic neurotransmitters, neuropeptides, calcium-binding proteins, and cell surface molecules. Cereb Cortex 3:273–289.

Dégenètais E, Thierry AM, Glowinski J, Gioanni Y (2003) Synaptic influence of hippocampus on pyramidal cells of the rat prefrontal cortex: an *in vivo* intracellular recording study. Cereb Cortex 13:782–792.

Destexhe A, Paré D (1999) Impact of network activity on the integrative properties of neocortical pyramidal neurons *in vivo*. J Neurophysiol 81:1531–1547.

Dumitriu D, Cossart R, Huang J, Yuste R (2007) Correlation between axonal morphologies and synaptic input kinetics of interneurons from mouse visual cortex. Cereb Cortex 17:81–91.

Engel AK, Singer W (2001) Temporal binding and the neural correlates of sensory awareness. Trends Cogn Sci 5:16–25.

Euston DR, Tatsuno M, McNaughton BL (2007) Fast-forward playback of recent memory sequences in prefrontal cortex during sleep. Science 318:1147–1150.

Ferino F, Thierry AM, Glowinski J (1987) Anatomical and electrophysiological evidence for a direct projection from Ammon's horn to the medial prefrontal cortex in the rat. Exp Brain Res 65:421–426.

Földy C, Dyhrfjeld-Johnsen J, Soltesz I (2005) Structure of cortical microcircuit theory. J Physiol 562:47–54.

Freund TF, Buzsáki G (1996) Interneurons of the hippocampus. Hippocampus 6:347–470.

Fuster JM (2001) The prefrontal cortex—an update: time is of the essence. Neuron 30:319–333.

Gabbott P, Headlam A, Busby S (2002) Morphological evidence that CA1 hippocampal afferents monosynaptically innervate PV-containing neurons and NADPH-diaphorase reactive cells in the medial prefrontal cortex (areas 25/32) of the rat. Brain Res 946:314–322.

Gabbott PL, Dickie BG, Vaid RR, Headlam AJ, Bacon SJ (1997) Local-circuit neurones in the medial prefrontal cortex (areas 25, 32 and 24b) in the rat: morphology and quantitative distribution. J Comp Neurol 377:465–499.

Gabernet L, Jadhav SP, Feldman DE, Carandini M, Scanziani M (2005) Somatosensory integration controlled by dynamic thalamocortical feed-forward inhibition. Neuron 48:315–327.

Galarreta M, Erdélyi F, Szabó G, Hestrin S (2008) Cannabinoid sensitivity and synaptic properties of 2 GABAergic networks in the neocortex. Cereb Cortex 18:2296–2305.

Giguere M, Goldman-Rakic PS (1988) Mediodorsal nucleus: areal, laminar, and tangential distribution of afferents and efferents in the frontal lobe of rhesus monkeys. J Comp Neurol 277:195–213.

Good P (2000) Permutation tests: a practical guide to resampling methods for testing hypotheses. New York: Springer.

Goto Y, Grace AA (2008) Dopamine modulation of hippocampal-prefrontal cortical interaction drives memory-guided behavior. Cereb Cortex 18:1407–1414.

Gupta A, Wang Y, Markram H (2000) Organizing principles for a diversity of GABAergic interneurons and synapses in the neocortex. Science 287:273–278.

Harris KD, Henze DA, Csicsvari J, Hirase H, Buzsáki G (2000) Accuracy of tetrode spike separation as determined by simultaneous intracellular and extracellular measurements. J Neurophysiol 84:401–414.

Hazan L, Zugaro M, Buzsáki G (2006) Klusters, NeuroScope, NDManager:

a free software suite for neurophysiological data processing and visualization. J Neurosci Methods 155:207–216.
Helmstaedter M, Sakmann B, Feldmeyer D (2009) L2/3 interneuron groups defined by multiparameter analysis of axonal projection, dendritic geometry, and electrical excitability. Cereb Cortex 19:951–962.
Hô N, Destexhe A (2000) Synaptic background activity enhances the responsiveness of neocortical pyramidal neurons. J Neurophysiol 84:1488–1496.
Hoover WB, Vertes RP (2007) Anatomical analysis of afferent projections to the medial prefrontal cortex in the rat. Brain Struct Funct 212:149–179.
Huguenard JR, McCormick DA (2007) Thalamic synchrony and dynamic regulation of global forebrain oscillations. Trends Neurosci 30:350–356.
Hyman JM, Zilli EA, Paley AM, Hasselmo ME (2005) Medial prefrontal cortex cells show dynamic modulation with the hippocampal theta rhythm dependent on behavior. Hippocampus 15:739–749.
Jay TM, Witter MP (1991) Distribution of hippocampal CA1 and subicular efferents in the prefrontal cortex of the rat studied by means of anterograde transport of *Phaseolus vulgaris*-leucoagglutinin. J Comp Neurol 313:574–586.
Jones BE (2008) Modulation of cortical activation and behavioral arousal by cholinergic and orexinergic systems. Ann N Y Acad Sci 1129:26–34.
Jones MW (2002) A comparative review of rodent prefrontal cortex and working memory. Curr Mol Med 2:639–647.
Jones MW, Wilson MA (2005) Theta rhythms coordinate hippocampal-prefrontal interactions in a spatial memory task. PLoS Biol 3:e402.
Jung MW, Wiener SI, McNaughton BL (1994) Comparison of spatial firing characteristics of units in dorsal and ventral hippocampus of the rat. J Neurosci 14:7347–7356.
Kapfer C, Glickfeld LL, Atallah BV, Scanziani M (2007) Supralinear increase of recurrent inhibition during sparse activity in the somatosensory cortex. Nat Neurosci 10:743–753.
Kawaguchi Y, Kubota Y (1997) GABAergic cell subtypes and their synaptic connections in rat frontal cortex. Cereb Cortex 7:476–486.
Kisvárday ZF, Tóth E, Rausch M, Eysel UT (1997) Orientation-specific relationship between populations of excitatory and inhibitory lateral connections in the visual cortex of the cat. Cereb Cortex 7:605–618.
Klausberger T, Somogyi P (2008) Neuronal diversity and temporal dynamics: the unity of hippocampal circuit operations. Science 321:53–57.
Klausberger T, Magill PJ, Márton LF, Roberts JD, Cobden PM, Buzsáki G, Somogyi P (2003) Brain-state- and cell-type-specific firing of hippocampal interneurons in vivo. Nature 421:844–848.
Koch C, Segev I (2000) The role of single neurons in information processing. Nat Neurosci 3 [Suppl]:1171–1177.
Krettek JE, Price JL (1977) The cortical projections of the mediodorsal nucleus and adjacent thalamic nuclei in the rat. J Comp Neurol 171:157–191.
Krimer LS, Zaitsev AV, Czanner G, Kröner S, González-Burgos G, Povysheva NV, Iyengar S, Barrionuevo G, Lewis DA (2005) Cluster analysis-based physiological classification and morphological properties of inhibitory neurons in layers 2–3 of monkey dorsolateral prefrontal cortex. J Neurophysiol 94:3009–3022.
Kröner S, Krimer LS, Lewis DA, Barrionuevo G (2007) Dopamine increases inhibition in the monkey dorsolateral prefrontal cortex through cell type-specific modulation of interneurons. Cereb Cortex 17:1020–1032.
Kuroda M, Yokofujita J, Oda S, Price JL (2004) Synaptic relationships between axon terminals from the mediodorsal thalamic nucleus and gamma-aminobutyric acidergic cortical cells in the prelimbic cortex of the rat. J Comp Neurol 477:220–234.
Lewis DA, Hashimoto T, Volk DW (2005) Cortical inhibitory neurons and schizophrenia. Nat Rev Neurosci 6:312–324.
Lubenov EV, Siapas AG (2008) Decoupling through synchrony in neuronal circuits with propagation delays. Neuron 58:118–131.
Markram H, Toledo-Rodriguez M, Wang Y, Gupta A, Silberberg G, Wu C (2004) Interneurons of the neocortical inhibitory system. Nat Rev Neurosci 5:793–807.
Maurer AP, Vanrhoads SR, Sutherland GR, Lipa P, McNaughton BL (2005) Self-motion and the origin of differential spatial scaling along the septo-temporal axis of the hippocampus. Hippocampus 15:841–852.
Miller EK (2000) The prefrontal cortex and cognitive control. Nat Rev Neurosci 1:59–65.
Mölle M, Marshall L, Gais S, Born J (2002) Grouping of spindle activity during slow oscillations in human non-rapid eye movement sleep. J Neurosci 22:10941–10947.
Molnár G, Oláh S, Komlósi G, Füle M, Szabadics J, Varga C, Barzó P, Tamás G (2008) Complex events initiated by individual spikes in the human cerebral cortex. PLoS Biol 6:e222.
Moser MB, Moser EI (1998) Functional differentiation in the hippocampus. Hippocampus 8:608–619.
Paxinos G, Watson C (2007) The rat brain in stereotaxic coordinates. San Diego: Academic.
Peters A, Palay SL (1991) The fine structure of the nervous system: neurons and their supporting cells. New York: Oxford UP.
Pinault D (1996) A novel single-cell staining procedure performed in vivo under electrophysiological control: morpho-functional features of juxtacellularly labeled thalamic cells and other central neurons with biocytin or neurobiotin. J Neurosci Methods 65:113–136.
Puig MV, Ushimaru M, Kawaguchi Y (2008) Two distinct activity patterns of fast-spiking interneurons during neocortical UP states. Proc Natl Acad Sci U S A 105:8428–8433.
Ranck JB Jr (1973) Studies on single neurons in dorsal hippocampal formation and septum in unrestrained rats. I. Behavioral correlates and firing repertoires. Exp Neurol 41:461–531.
Rotaru DC, Barrionuevo G, Sesack SR (2005) Mediodorsal thalamic afferents to layer III of the rat prefrontal cortex: synaptic relationships to subclasses of interneurons. J Comp Neurol 490:220–238.
Sanchez-Vives MV, McCormick DA (2000) Cellular and network mechanisms of rhythmic recurrent activity in neocortex. Nat Neurosci 3:1027–1034.
Siapas AG, Wilson MA (1998) Coordinated interactions between hippocampal ripples and cortical spindles during slow-wave sleep. Neuron 21:1123–1128.
Siapas AG, Lubenov EV, Wilson MA (2005) Prefrontal phase locking to hippocampal theta oscillations. Neuron 46:141–151.
Sirota A, Csicsvari J, Buhl D, Buzsáki G (2003) Communication between neocortex and hippocampus during sleep in rodents. Proc Natl Acad Sci U S A 100:2065–2069.
Sirota A, Montgomery S, Fujisawa S, Isomura Y, Zugaro M, Buzsáki G (2008) Entrainment of neocortical neurons and gamma oscillations by the hippocampal theta rhythm. Neuron 60:683–697.
Skaggs WE, McNaughton BL, Wilson MA, Barnes CA (1996) Theta phase precession in hippocampal neuronal populations and the compression of temporal sequences. Hippocampus 6:149–172.
Somogyi P, Klausberger T (2005) Defined types of cortical interneurone structure space and spike timing in the hippocampus. J Physiol 562:9–26.
Steriade M, Deschênes M, Domich L, Mulle C (1985) Abolition of spindle oscillations in thalamic neurons disconnected from nucleus reticularis thalami. J Neurophysiol 54:1473–1497.
Steriade M, Domich L, Oakson G, Deschênes M (1987) The deafferented reticular thalamic nucleus generates spindle rhythmicity. J Neurophysiol 57:260–273.
Steriade M, McCormick DA, Sejnowski TJ (1993) Thalamocortical oscillations in the sleeping and aroused brain. Science 262:679–685.
Swadlow HA, Beloozerova IN, Sirota MG (1998) Sharp, local synchrony among putative feed-forward inhibitory interneurons of rabbit somatosensory cortex. J Neurophysiol 79:567–582.
Swanson LW (1981) A direct projection from Ammon's horn to prefrontal cortex in the rat. Brain Res 217:150–154.
Szabadics J, Tamás G, Soltesz I (2007) Different transmitter transients underlie presynaptic cell type specificity of GABAA, slow and GABAA, fast. Proc Natl Acad Sci U S A 104:14831–14836.
Tamás G, Szabadics J, Lörincz A, Somogyi P (2004) Input and frequency-specific entrainment of postsynaptic firing by IPSPs of perisomatic or dendritic origin. Eur J Neurosci 20:2681–2690.
Tierney PL, Dégenètais E, Thierry AM, Glowinski J, Gioanni Y (2004) Influence of the hippocampus on interneurons of the rat prefrontal cortex. Eur J Neurosci 20:514–524.
Tierney PL, Thierry AM, Glowinski J, Deniau JM, Gioanni Y (2008) Dopamine modulates temporal dynamics of feedforward inhibition in rat prefrontal cortex *in vivo*. Cereb Cortex 18:2251–2262.
Tukker JJ, Fuentealba P, Hartwich K, Somogyi P, Klausberger T (2007) Cell type-specific tuning of hippocampal interneuron firing during gamma oscillations *in vivo*. J Neurosci 27:8184–8189.
Vertes RP (2006) Interactions among the medial prefrontal cortex, hippocampus and midline thalamus in emotional and cognitive processing in the rat. Neuroscience 142:1–20.
Zar JH (1999) Biostatistical analysis. Upper Saddle River, NJ: Prentice Hall.

Supplemental Table 1

antibody to	host	dilution	source	reference of characterization and specificity
CB	rabbit	1:5000	Swant, Bellinzona, Switzerland, code no 38	labelling patterns as published with other antibodies
CCK	mouse	1:5000	*Dr. G. Ohning, CURE, UCLA, USA, Code 9303	(Ohning et al., 1996)
	rabbit	1:1000	pro-CCK; Dr. G. Dockrey, Liverpool University, UK, code no L424	(Morino et al., 1994)
GAD	mouse	1:500	Millipore Corporation , Billerica, USA, code no MAB 351, Lot 21111355	(Chang and Gottlieb, 1988)
	mouse	1:100	Dev.Stu.Hybr. Bank, Univ. Iowa, code GAD-6	(Chang and Gottlieb, 1988)
PV	mouse	1:5000	Swant,Bellinzona, Switzerland, code no 235	(Celio et al., 1988)
	guinea pig	1:2000	Dr. K.G. Baimbridge, Dept. Physiol., Univ. British Columbia, Canada, Code no 404	labelling patterns as published with other antibodies and K.G.B. personal communication
SOM	mouse	1:300	Dr. A. Buchan, Dept. Physiol., Univ. Br. Columbia, Canada, code no mAb Soma8	(Vincent et al., 1985)
	rat	1:500	Millipore Corporation , Billerica, USA, code no MAB 354	labelling patterns as published with other antibodies
VIP	mouse	1:100000	*Dr. G. Ohning, CURE, UCLA, USA, Code 55	(Wong et al., 1996)

*Antibodies by CURE/Digestive Diseases Research Center, Antibody/RIA Core, UCLA, NIH Grant #DK 41301

Reference List

Celio MR, Baier W, Scharer L, de Viragh PA, Gerday C (1988) Monoclonal antibodies directed against the calcium binding protein parvalbumin. Cell Calcium 9:81-86.

Chang YC, Gottlieb DI (1988) Characterization of the proteins purified with monoclonal antibodies to glutamic acid decarboxylase. J Neurosci 8:2123-2130.

Morino P, Herrera-Marschitz M, Castel MN, Ungerstedt U, Varro A, Dockray G, Hokfelt T (1994) Cholecystokinin in cortico-striatal neurons in the rat: immunohistochemical studies at the light and electron microscopical level. Eur J Neurosci 6:681-692.

Ohning GV, Wong HC, Lloyd KC, Walsh JH (1996) Gastrin mediates the gastric mucosal proliferative response to feeding. Am J Physiol 271:G470-G476.

Vincent SR, McIntosh CH, Buchan AM, Brown JC (1985) Central somatostatin systems revealed with monoclonal antibodies. pp 169-186.

Wong HC, Sternini C, Lloyd K, De GR, Walsh JH (1996) Monoclonal antibody to VIP: production, characterization, immunoneutralizing activity, and usefulness in cytochemical staining. Hybridoma 15:133-139.

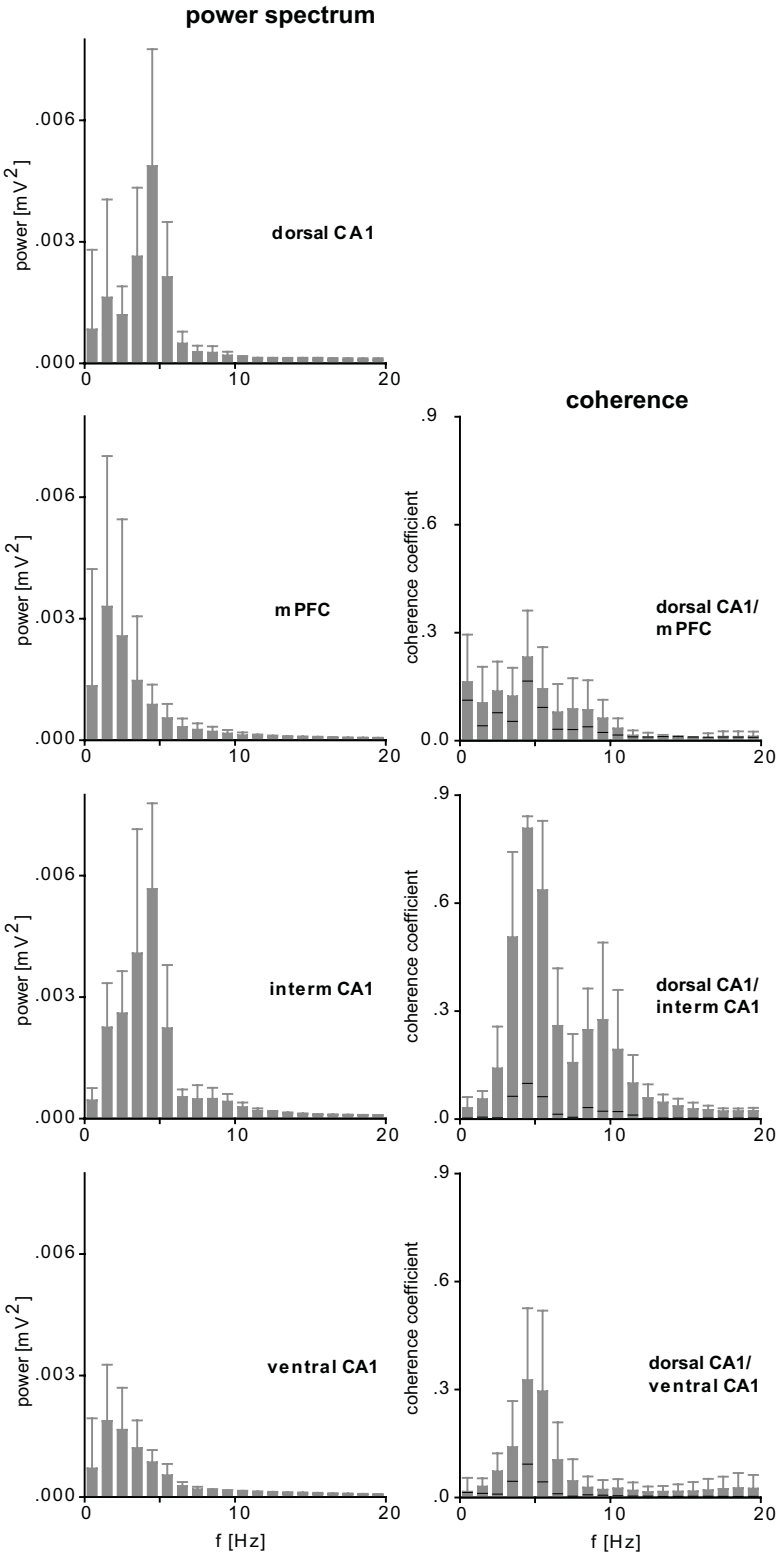

suppl Fig 1. Hartwich et al. (2008)

Suppl. Figure 1. Power and coherence of theta oscillations in the mPFC, dorsal, intermediate and ventral CA1 hippocampus. Bars represent mean and SD from the indicated number of recordings. **A,** Power spectra of the LFP in the dorsal CA1 (n=33 recordings), mPfC (n=17 recordings), intermediate CA1 (n=6 recordings) and ventral CA1 area (n=10 recordings) during theta oscillations detected in the dorsal CA1 hippocampus. Note the prominent peak at 4 Hz in the dorsal and intermediate hippocampus. In the mPFC and ventral hippocampus 4 Hz theta oscillations are present but the dominant frequency is in the 2 Hz band. **B,** Coherence spectrum between local field potentials in the dorsal CA1 hippocampus and mPFC (n=17 recordings), intermediate CA1 (n=6 recordings) or ventral CA1 hippocampus (n=10 recordings) during theta oscillations detected in the dorsal CA1 hippocampus. Note the prominent peak at 4 Hz in all plots. However, the coherence in the theta band is higher between the dorsal and intermediate CA1 in comparison to dorsal CA1 and mPFC or ventral CA1. Black lines indicate significance thresholds determined by shuffling as described in the Methods.

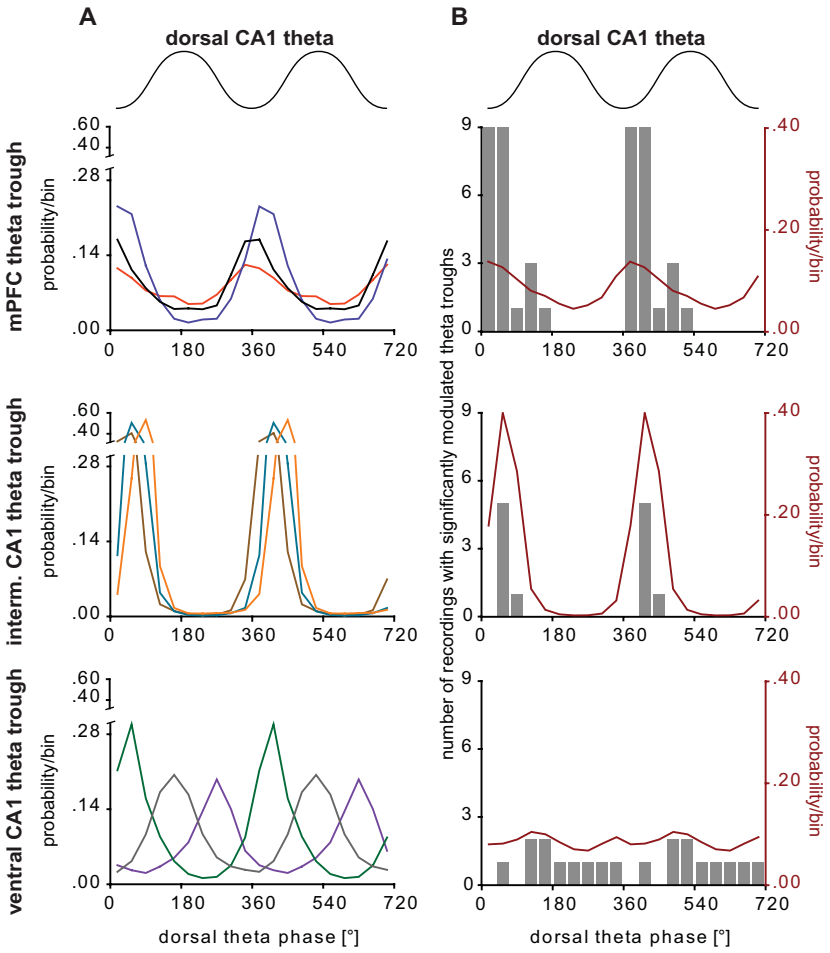

suppl Fig 2. Hartwich et al. (2008)

Suppl. Figure 2. Theta phase relationships between the dorsal CA1 hippocampus and the mPFC, intermediate or ventral CA1 area. **A, B,** Upper schematic waveform indicates two dorsal CA1 theta cycles; 0° and 360° mark the troughs. **A,** Phase probability of troughs detected from the filtered LFP (3-6 Hz) of the mPFC (upper graph), intermediate CA1 (middle graph) and ventral CA1 (lower graph) to the dorsal CA1 theta cycle (bin size 36°). Only those troughs with an inter-event time between 0.167 and 0.333 s were considered. Colored traces show examples of individual recordings. **B,** The grey columns and left y-axis indicate the number of recordings observed with a significant mean theta phase. The red curve and right y-axis indicate the mean trough probability of all recordings in a particular area. In the mPFC in 3 out of 26 recordings no significant modulation of the theta troughs in relation to dorsal CA1 theta oscillations could be detected. Note that theta troughs in the mPFC are slightly delayed in relation to dorsal CA1 theta oscillations and theta troughs in the intermediate CA1 area are in phase with the dorsal CA1 theta troughs. Theta troughs from individual recordings in the ventral CA1 area are phase coupled to dorsal CA1 theta oscillations. However, the preferred theta trough phase is highly heterogeneous between different recording sites. Because putative pyramidal cells in the ventral CA1 area were phase coupled to the same dorsal CA1 theta phase (peak) irrespective of the recording site, this suggests that theta oscillations in the ventral CA1 hippocampus might be strongly influenced by volume conduction due to its own curvature and the geometry of the surrounding structures, which may also oscillate at theta frequency.

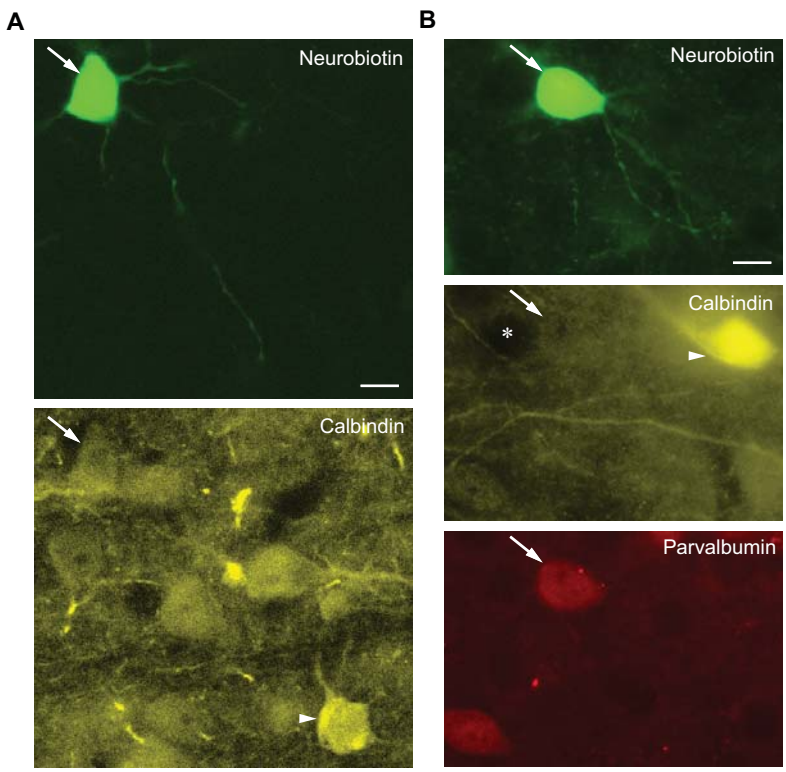

suppl Fig 3. Hartwich et al (2008)

Suppl. Figure 3. Basket cells in the PL cortex are immunopositive for PV and CB. **A,** A neurobiotin labeled soma of a basket cell (K 101a) is weakly immunopositive for calbindin (arrow) compared to strong immunopositive CB cells (arrowhead) nearby. **B,** Immunofluorescence micrographs showing a neurobiotin labeled soma of a basket cell (K124a) weakly immunopositive for calbindin compared to a negative soma (star) and strong positive soma (arrowhead) nearby. The soma of this cell was also tested positive for PV. **Scale bars:** 10 µm.